Appendix A
Observational Datasets Used in Climate Studies

Recommended Citation for Chapter

Wuebbles, D.J., 2017: Observational datasets used in climate studies. In: *Climate Science Special Report: Fourth National Climate Assessment, Volume I* [Wuebbles, D.J., D.W. Fahey, K.A. Hibbard, D.J. Dokken, B.C. Stewart, and T.K. Maycock (eds.)]. U.S. Global Change Research Program, Washington, DC, USA, pp. 430-435, doi: 10.7930/J0BK19HT.

Climate Datasets

Observations, including those from satellites, mobile platforms, field campaigns, and ground-based networks, provide the basis of knowledge on many temporal and spatial scales for understanding the changes occurring in Earth's climate system. These observations also inform the development, calibration, and evaluation of numerical models of the physics, chemistry, and biology being used in analyzing past changes in climate and for making future projections. As all observational data collected by support from Federal agencies are required to be made available free of charge with machine readable metadata, everyone can access these products for their personal analysis and research and for informing decisions. Many of these datasets are accessible through web services.

Many long-running observations worldwide have provided us with long-term records necessary for investigating climate change and its impacts. These include important climate variables such as surface temperature, sea ice extent, sea level rise, and streamflow. Perhaps one of the most iconic climatic datasets, that of atmospheric carbon dioxide measured at Mauna Loa, Hawai'i, has been recorded since the 1950s. The U.S. and Global Historical Climatology Networks have been used as authoritative sources of recorded surface temperature increases, with some stations having continuous records going back many decades. Satellite radar altimetry data (for example, TOPEX/JASON1 & 2 satellite data) have informed the development of the University of Colorado's 20+ year record of global sea level changes. In the United States, the USGS (U.S. Geological Survey) National Water Information System contains, in some instances, decades of daily streamflow records which inform not only climate but land-use studies as well. The U.S. Bureau of Reclamation and U.S. Army Corp of Engineers have maintained data about reservoir levels for decades where applicable. Of course, datasets based on shorter-term observations are used in conjunction with longer-term records for climate study, and the U.S. programs are aimed at providing continuous data records. Methods have been developed and applied to process these data so as to account for biases, collection method, earth surface geometry, the urban heat island effect, station relocations, and uncertainty (e.g., see Vose et al. 2012;[1] Rennie et al. 2014;[2] Karl et al. 2015[3]).

Even observations not designed for climate have informed climate research. These include ship logs containing descriptions of ice extent, readings of temperature and precipitation provided in newspapers, and harvest records. Today, observations recorded both manually and in automated fashions inform research and are used in climate studies.

The U.S Global Change Research Program (USGCRP) has established the Global Change Information System (GCIS) to better coordinate and integrate the use of federal information products on changes in the global environment and the implications of those changes for society. The GCIS is an open-source, web-based resource for traceable global change data, information, and products. Designed for use by scientists, decision makers, and the public, the GCIS provides coordinated links to a select group of information products produced, maintained, and disseminated by government agencies and organizations. Currently the GCIS is aimed at the datasets used in Third National Climate Assessment (NCA3) and the USGCRP Climate and Health Assessment. It will be updated for the datasets used in this report (The Climate Science Special Report, CSSR).

Temperature and Precipitation Observational Datasets

For analyses of surface temperature or precipitation, including determining changes over the globe or the United States, the starting point is accumulating observations of surface air temperature or precipitation taken at observing stations all over the world, and, in the case of temperature, sea surface temperatures (SSTs) taken by ships and buoys. These are direct measurements of the air temperature, sea surface temperature, and precipitation. The observations are quality assured to exclude clearly erroneous values. For temperature, additional analyses are performed on the data to correct for known biases in the way the temperatures were measured. These biases include the change to the observations that result from changes in observing practices or changes in the location or local environment of an observing station. One example is with SSTs where there was a change in practice from throwing a bucket over the side of the ship, pulling up seawater and measuring the temperature of the water in the bucket to measuring the temperature of the water in the engine intake. The bucket temperatures are systematically cooler than engine intake water and must be corrected.

For evaluating the globally averaged temperature, data are then compared to a long-term average for the location where the observations were taken (e.g., a 30-year average for an individual observing station) to create a deviation from that average, commonly referred to as an anomaly. Using anomalies allows the spatial averaging of stations in different climates and elevations to produce robust estimates of the spatially averaged temperature or precipitation for a given area.

To calculate the temperature or precipitation for a large area, like the globe or the United States, the area is divided into "grid boxes" usually in latitude/longitude space. For example, one common grid size has 5° x 5° latitude/longitude boxes, where each side of a grid box is 5° of longitude and 5° of latitude in length. All data anomalies in a given grid box are averaged together to produce a gridbox average. Some grid boxes contain no observations, but nearby grid boxes do contain observations, so temperatures or precipitation for the grid boxes with no observations are estimated as a function of the nearby grid boxes with observations for that date.

Calculating the temperature or precipitation value for the larger area, either the globe or the United States, is done by averaging the values for all the grid boxes to produce one number for each day, month, season, or year resulting in a time series. The time series in each of the grid boxes are also used to calculate long-term trends in the temperature or precipitation for each grid box. This provides a picture of how temperatures and precipitation are changing in different locations.

Evidence for changes in the climate of the United States arises from multiple analyses of data from *in situ*, satellite, and other records undertaken by many groups over several decades. The primary dataset for surface temperatures and precipitation in the United States is nClimGrid,[4, 5] though trends are similar in the U.S. Historical Climatology Network, the Global Historical Climatology Network, and other datasets. For temperature, several atmospheric reanalyses (e.g., 20th Century Reanalysis, Climate Forecast System Reanalysis, ERA-Interim, and Modern Era Reanalysis for Research and Applications) confirm rapid warming at the surface since 1979, with observed trends closely tracking the ensemble mean of the reanalyses.[1] Several recently improved satellite datasets document changes in middle tropospheric temperatures.[6, 7, 8] Longer-term changes are depicted using multiple paleo analyses (e.g., Wahl and Smerdon 2012;[9] Trouet et al. 2013[10]).

Satellite Temperature Datasets

A special look is given to the satellite temperature datasets because of controversies associated with these datasets. Satellite-borne microwave sounders such as the Microwave Sounding Unit (MSU) and Advanced Microwave Sounding Unit (AMSU) instruments operating on NOAA polar-orbiting platforms take measurements of the temperature of thick layers of the atmosphere with near global coverage. Because the long-term data record requires the piecing together of measurements made by 16 different satellites, accurate instrument intercalibration is of critical importance. Over the mission lifetime of most satellites, the instruments drift in both calibration and local measurement time. Adjustments to counter the effects of these drifts need to be developed and applied before a long-term record can be assembled. For tropospheric measurements,

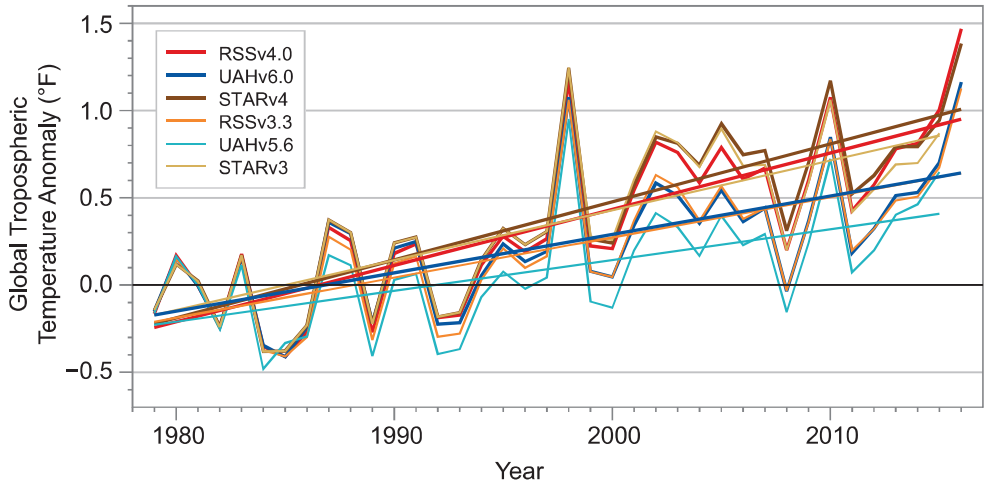

Figure A.1: Annual global (80°S–80°N) mean time series of tropospheric temperature for five recent datasets (see below). Each time series is adjusted so the mean value for the first three years is zero. This accentuates the differences in the long-term changes between the datasets. (Figure source: Remote Sensing Systems).

Table A.1.: Global Trends in Temperature Total Troposphere (TTT) since 1979 and 2000 (in °F per decade).

Dataset	Trend (1979–2015) (°F/Decade)	Trend (2000–2015) (°F/Decade)
RSS V4.0	0.301	0.198
UAH V6Beta5	0.196	0.141
STAR V4.0	0.316	0.157
RSS V3.3	0.208	0.105
UAH V5.6	0.176	0.211
STAR V3.0	0.286	0.061

the most challenging of these adjustments is the adjustment for drifting measurement time, which requires knowledge of the diurnal cycle in both atmospheric and surface temperature. Current versions of the sounder-based datasets account for the diurnal cycle by either using diurnal cycles deduced from model output[11, 12] or by attempting to derive the diurnal cycle from the satellite measurements themselves (an approach plagued by sampling issues and possible calibration drifts).[13, 14] Recently a hybrid approach has been developed, RSS Version 4.0,[6] that results in an increased warming signal relative to the other approaches, particularly since 2000. Each of these methods has strengths and weaknesses, but none has sufficient accuracy to construct an unassailable long-term record of atmospheric temperature change. The resulting datasets show a greater spread in decadal-scale trends than do the surface temperature datasets for the same period, suggesting that they may be less reliable. Figure A.1 shows annual time series for the global mean tropospheric temperature for some recent versions of the satellite datasets. These data have been adjusted to remove the influence of stratospheric cooling.[15] Linear trend values are shown in Table A.1.

DATA SOURCES

All Satellite Data are "Temperature Total Troposphere" time series calculated from TMT and TLS

(1.1*TMT) - (0.1*TLS). This combination reduces the effect of the lower stratosphere on the tropospheric temperature. (Fu, Qiang et al. "Contribution of stratospheric cooling to satellite-inferred tropospheric temperature trends." *Nature* 429.6987 (2004): 55-58.)

UAH. UAH Version 6.0Beta5. Yearly (yyyy) text files of TMT and TLS are available from

https://www.nsstc.uah.edu/data/msu/v6.0beta/tmt/

https://www.nsstc.uah.edu/data/msu/v6.0beta/tls/

Downloaded 5/15/2016.

UAH. UAH Version 5.6. Yearly (yyyy) text files of TMT and TLS are available from

http://vortex.nsstc.uah.edu/data/msu/t2/

http://vortex.nsstc.uah.edu/data/msu/t4/

Downloaded 5/15/2016.

RSS. RSS Version 4.0.

ftp://ftp.remss.com/msu/data/netcdf/RSS_Tb_Anom_Maps_ch_TTT_V4_0.nc

Downloaded 5/15/2016

RSS. RSS Version 3.3.

ftp://ftp.remss.com/msu/data/netcdf/RSS_Tb_Anom_Maps_ch_TTT_V3.3.nc

Downloaded 5/15/2016

NOAA STAR. Star Version 3.0.

ftp://ftp.star.nesdis.noaa.gov/pub/smcd/emb/mscat/data/MSU_AMSU_v3.0/Monthly_Atmospheric_Layer_Mean_Temperature/Merged_Deep-Layer_Temperature/NESDIS-STAR_TCDR_MSU-AMSUA_V03R00_TMT_S197811_E201709_C20171002.nc

ftp://ftp.star.nesdis.noaa.gov/pub/smcd/emb/mscat/data/MSU_AMSU_v3.0/Monthly_Atmospheric_Layer_Mean_Temperature/Merged_Deep-Layer_Temperature/NESDIS-STAR_TCDR_MSU-AMSUA_V03R00_TLS_S197811_E201709_C20171002.nc

Downloaded 5/18/2016.

REFERENCES

1. Vose, R.S., D. Arndt, V.F. Banzon, D.R. Easterling, B. Gleason, B. Huang, E. Kearns, J.H. Lawrimore, M.J. Menne, T.C. Peterson, R.W. Reynolds, T.M. Smith, C.N. Williams, and D.L. Wuertz, 2012: NOAA's merged land-ocean surface temperature analysis. *Bulletin of the American Meteorological Society*, **93**, 1677-1685. http://dx.doi.org/10.1175/BAMS-D-11-00241.1

2. Rennie, J.J., J.H. Lawrimore, B.E. Gleason, P.W. Thorne, C.P. Morice, M.J. Menne, C.N. Williams, Jr., W.G. de Almeida, J.R. Christy, M. Flannery, M. Ishihara, K. Kamiguchi, A.M.G. Klein-Tank, A. Mhanda, D.H. Lister, V. Razuvaev, M. Renom, M. Rusticucci, J. Tandy, S.J. Worley, V. Venema, W. Angel, M. Brunet, B. Dattore, H. Diamond, M.A. Lazzara, F. Le Blancq, J. Luterbacher, H. Mächel, J. Revadekar, R.S. Vose, and X. Yin, 2014: The international surface temperature initiative global land surface databank: Monthly temperature data release description and methods. *Geoscience Data Journal*, **1**, 75-102. http://dx.doi.org/10.1002/gdj3.8

3. Karl, T.R., A. Arguez, B. Huang, J.H. Lawrimore, J.R. McMahon, M.J. Menne, T.C. Peterson, R.S. Vose, and H.-M. Zhang, 2015: Possible artifacts of data biases in the recent global surface warming hiatus. *Science*, **348**, 1469-1472. http://dx.doi.org/10.1126/science.aaa5632

4. Vose, R.S., S. Applequist, M. Squires, I. Durre, M.J. Menne, C.N. Williams, Jr., C. Fenimore, K. Gleason, and D. Arndt, 2014: Improved historical temperature and precipitation time series for U.S. climate divisions. *Journal of Applied Meteorology and Climatology*, **53**, 1232-1251. http://dx.doi.org/10.1175/JAMC-D-13-0248.1

5. Vose, R.S., M. Squires, D. Arndt, I. Durre, C. Fenimore, K. Gleason, M.J. Menne, J. Partain, C.N. Williams Jr., P.A. Bieniek, and R.L. Thoman, 2017: Deriving historical temperature and precipitation time series for Alaska climate divisions via climatologically aided interpolation. *Journal of Service Climatology* **10**, 20. https://www.stateclimate.org/sites/default/files/upload/pdf/journal-articles/2017-Ross-etal.pdf

6. Mears, C.A. and F.J. Wentz, 2016: Sensitivity of satellite-derived tropospheric temperature trends to the diurnal cycle adjustment. *Journal of Climate*, **29**, 3629-3646. http://dx.doi.org/10.1175/JCLI-D-15-0744.1

7. Spencer, R.W., J.R. Christy, and W.D. Braswell, 2017: UAH Version 6 global satellite temperature products: Methodology and results. *Asia-Pacific Journal of Atmospheric Sciences*, **53**, 121-130. http://dx.doi.org/10.1007/s13143-017-0010-y

8. Zou, C.-Z. and J. Li, 2014: NOAA MSU Mean Layer Temperature. National Oceanic and Atmospheric Administration, Center for Satellite Applications and Research, 35 pp. http://www.star.nesdis.noaa.gov/smcd/emb/mscat/documents/MSU_TCDR_CATBD_Zou_Li.pdf

9. Wahl, E.R. and J.E. Smerdon, 2012: Comparative performance of paleoclimate field and index reconstructions derived from climate proxies and noise-only predictors. *Geophysical Research Letters*, **39**, L06703. http://dx.doi.org/10.1029/2012GL051086

10. Trouet, V., H.F. Diaz, E.R. Wahl, A.E. Viau, R. Graham, N. Graham, and E.R. Cook, 2013: A 1500-year reconstruction of annual mean temperature for temperate North America on decadal-to-multidecadal time scales. *Environmental Research Letters*, **8**, 024008. http://dx.doi.org/10.1088/1748-9326/8/2/024008

11. Mears, C.A. and F.J. Wentz, 2009: Construction of the Remote Sensing Systems V3.2 atmospheric temperature records from the MSU and AMSU microwave sounders. *Journal of Atmospheric and Oceanic Technology*, **26**, 1040-1056. http://dx.doi.org/10.1175/2008JTECHA1176.1

12. Zou, C.-Z., M. Gao, and M.D. Goldberg, 2009: Error structure and atmospheric temperature trends in observations from the microwave sounding unit. *Journal of Climate*, **22**, 1661-1681. http://dx.doi.org/10.1175/2008JCLI2233.1

13. Christy, J.R., R.W. Spencer, W.B. Norris, W.D. Braswell, and D.E. Parker, 2003: Error estimates of version 5.0 of MSU–AMSU bulk atmospheric temperatures. *Journal of Atmospheric and Oceanic Technology*, **20**, 613-629. http://dx.doi.org/10.1175/1520-0426(2003)20<613:EEOVOM>2.0.CO;2

14. Po-Chedley, S., T.J. Thorsen, and Q. Fu, 2015: Removing diurnal cycle contamination in satellite-derived tropospheric temperatures: Understanding tropical tropospheric trend discrepancies. *Journal of Climate*, **28**, 2274-2290. http://dx.doi.org/10.1175/JCLI-D-13-00767.1

15. Fu, Q. and C.M. Johanson, 2005: Satellite-derived vertical dependence of tropical tropospheric temperature trends. *Geophysical Research Letters*, **32**, L10703. http://dx.doi.org/10.1029/2004GL022266

Appendix B
Model Weighting Strategy

Recommended Citation for Chapter

Sanderson, B.M. and M.F. Wehner, 2017: Model weighting strategy. In: *Climate Science Special Report: Fourth National Climate Assessment, Volume I* [Wuebbles, D.J., D.W. Fahey, K.A. Hibbard, D.J. Dokken, B.C. Stewart, and T.K. Maycock (eds.)]. U.S. Global Change Research Program, Washington, DC, USA, pp. 436-442, doi: 10.7930/J06T0JS3.

Introduction

This document briefly describes a weighting strategy for use with the Climate Model Intercomparison Project, Phase 5 (CMIP5) multimodel archive in the Fourth National Climate Assessment (NCA4). This approach considers both skill in the climatological performance of models over North America and the interdependency of models arising from common parameterizations or tuning practices. The method exploits information relating to the climatological mean state of a number of projection-relevant variables as well as long-term metrics representing long-term statistics of weather extremes. The weights, once computed, can be used to simply compute weighted mean and significance information from an ensemble containing multiple initial condition members from co-dependent models of varying skill.

Our methodology is based on the concepts outlined in Sanderson et al. 2015,[1] and the specific application to the NCA4 is also described in that paper. The approach produces a single set of model weights that can be used to combine projections into a weighted mean result, with significance estimates which also treat the weighting appropriately.

The method, ideally, would seek to have two fundamental characteristics:

- If a duplicate of one ensemble member is added to the archive, the resulting mean and significance estimate for future change computed from the ensemble should not change.

- If a demonstrably unphysical model is added to the archive, the resulting mean and significance estimates should also not change.

Method

The analysis requires an assessment of both model skill and an estimate of intermodel relationships—for which intermodel root mean square difference is taken as a proxy. The model and observational data used here is for the contiguous United States (CONUS), and most of Canada, using high-resolution data where available. Intermodel distances are computed as simple root mean square differences. Data is derived from a number of mean state fields and a number of fields that represent extreme behavior—these are listed in Table B.1. All fields are masked to only include information from CONUS/Canada.

The root mean square error (RMSE) between observations and each model can be used to produce an overall ranking for model simulations of the North American climate. Figure B.1 shows how this metric is influenced by different component variables.

Table B.1: Observational datasets used as observations.

Field	Description	Source	Reference	Years
TS	Surface Temperature (seasonal)	Livneh, Hutchinson	(Hopkinson et al. 2012;[3] Hutchinson et al. 2009;[4] Livneh et al. 2013[5])	1950–2011
PR	Mean Precipitation (seasonal)	Livneh, Hutchinson	(Hopkinson et al. 2012;[3] Hutchinson et al. 2009;[4] Livneh et al. 2013[5])	1950–2011
RSUT	TOA Shortwave Flux (seasonal)	CERES-EBAF	(Wielicki et al. 1996[6])	2000–2005
RLUT	TOA Longwave Flux (seasonal)	CERES-EBAF	(Wielicki et al. 1996[6])	2000–2005
T	Vertical Temperature Profile (seasonal)	AIRS*	(Aumann et al. 2003[7])	2002–2010
RH	Vertical Humidity Profile (seasonal)	AIRS	(Aumann et al. 2003[7])	2002–2010
PSL	Surface Pressure (seasonal)	ERA-40	(Uppala et al. 2005[8])	1970–2000
Tnn	Coldest Night	Livneh, Hutchinson	(Hopkinson et al. 2012;[3] Hutchinson et al. 2009;[4] Livneh et al. 2013[5])	1950–2011
Txn	Coldest Day	Livneh, Hutchinson	(Hopkinson et al. 2012;[3] Hutchinson et al. 2009;[4] Livneh et al. 2013[5])	1950–2011
Tnx	Warmest Night	Livneh, Hutchinson	(Hopkinson et al. 2012;[3] Hutchinson et al. 2009;[4] Livneh et al. 2013[5])	1950–2011
Txx	Warmest day	Livneh, Hutchinson	(Hopkinson et al. 2012;[3] Hutchinson et al. 2009;[4] Livneh et al. 2013[5])	1950–2011
rx5day	seasonal max. 5-day total precip.	Livneh, Hutchinson	(Hopkinson et al. 2012;[3] Hutchinson et al. 2009;[4] Livneh et al. 2013[5])	1950–2011

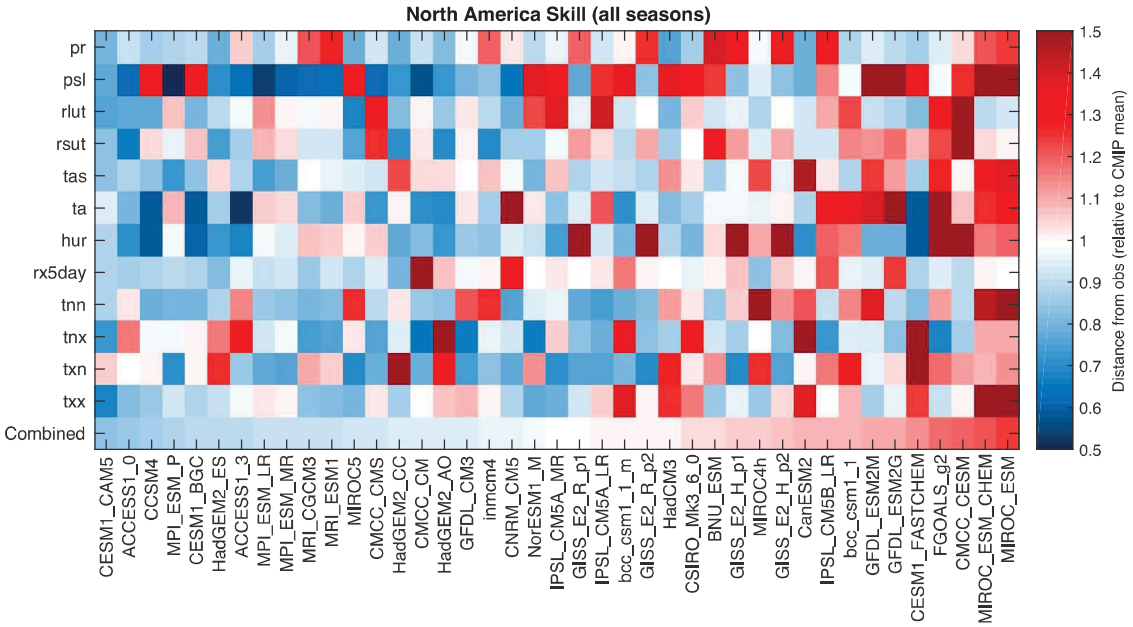

Figure B.1: A graphical representation of the intermodel distance matrix for CMIP5 and a set of observed values. Each row and column represents a single climate model (or observation). All scores are aggregated over seasons (individual seasons are not shown). Each box represents a pairwise distance, where warm (red) colors indicate a greater distance. Distances are measured as a fraction of the mean intermodel distance in the CMIP5 ensemble. (Figure source: Sanderson et al. 2017[2]).

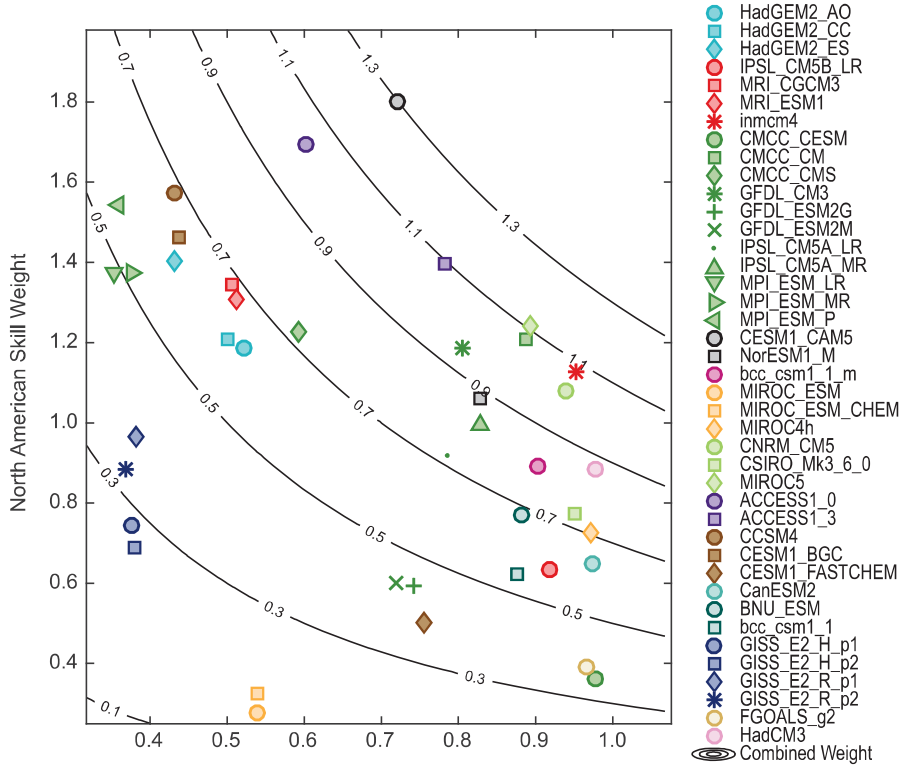

Figure B.2: Model skill and independence weights for the CMIP5 archive evaluated over the North American domain. Contours show the overall weighting, which is the product of the two individual weights. (Figure source: Sanderson et al. 2017[2]).

Models are downweighted for poor skill if their multivariate combined error is significantly greater than a "skill radius" term, which is a free parameter of the approach. The calibration of this parameter is determined through a perfect model study.[2] A pairwise distance matrix is computed to assess intermodel RMSE values for each model pair in the archive, and a model is downweighted for dependency if there exists another model with a pairwise distance to the original model significantly smaller than a "similarity radius." This is the second parameter of the approach, which is calibrated by considering known relationships within the archive. The resulting skill and independence weights are multiplied to give an overall "combined" weight—illustrated in Figure B.2 for the CMIP5 ensemble and listed in Table B.2.

The weights are used in the Climate Science Special Report (CSSR) to produce weighted mean and significance maps of future change, where the following protocol is used:

- Stippling—large changes, where the weighted multimodel average change is greater than double the standard deviation of the 20-year mean from control simulations runs, and 90% of the weight corresponds to changes of the same sign.

- Hatching—No significant change, where the weighted multimodel average change is less than the standard deviation of the 20-year means from control simulations runs.

- Whited out—Inconclusive, where the weighted multimodel average change is greater than double the standard deviation of the 20-year mean from control runs and less than 90% of the weight corresponds to changes of the same sign.

We illustrate the application of this method to future projections of precipitation change under the higher scenario (RCP8.5) in Figure B.3. The weights used in the report are chosen to be conservative, minimizing the risk of overconfidence and maximizing out-of-sample predictive skill for future projections. This results (as in Figure B.3) in only modest differences in the weighted and unweighted maps. It is shown in Sanderson et al. 2017[2] that a more aggressive weighting strategy, or one focused on a particular variable, tends to exhibit a stronger constraint on future change relative to the unweighted case. It is also notable that tradeoffs exist between skill and replication in the archive (evident in Figure B.2), such that the weighting for both skill and uniqueness has a compensating effect. As such, mean projections using the CMIP5 ensemble are not strongly influenced by the weighting. However, the establishment of the weighting strategy used in the CSSR provides some insurance against a potential case in future assessments where there is a highly replicated, but poorly performing model.

Table B.2: Uniqueness, skill, and combined weights for CMIP5.

	Uniqueness Weight	Skill Weight	Combined
ACCESS1-0	0.60	1.69	1.02
ACCESS1-3	0.78	1.40	1.09
BNU-ESM	0.88	0.77	0.68
CCSM4	0.43	1.57	0.68
CESM1-BGC	0.44	1.46	0.64
CESM1-CAM5	0.72	1.80	1.30
CESM1-FASTCHEM	0.76	0.50	0.38
CMCC-CESM	0.98	0.36	0.35
CMCC-CM	0.89	1.21	1.07
CMCC-CMS	0.59	1.23	0.73
CNRM-CM5	0.94	1.08	1.01
CSIRO-Mk3-6-0	0.95	0.77	0.74
CanESM2	0.97	0.65	0.63
FGOALS-g2	0.97	0.39	0.38
GFDL-CM3	0.81	1.18	0.95
GFDL-ESM2G	0.74	0.59	0.44
GFDL-ESM2M	0.72	0.60	0.43
GISS-E2-H-p1	0.38	0.74	0.28
GISS-E2-H-p2	0.38	0.69	0.26
GISS-E2-R-p1	0.38	0.97	0.37
GISS-E2-R-p2	0.37	0.89	0.33
HadCM3	0.98	0.89	0.87
HadGEM2-AO	0.52	1.19	0.62
HadGEM2-CC	0.50	1.21	0.60
HadGEM2-ES	0.43	1.40	0.61
IPSL-CM5A-LR	0.79	0.92	0.72
IPSL-CM5A-MR	0.83	0.99	0.82
IPSL-CM5B-LR	0.92	0.63	0.58
MIROC-ESM	0.54	0.28	0.15
MIROC-ESM-CHEM	0.54	0.32	0.17
MIROC4h	0.97	0.73	0.71
MIROC5	0.89	1.24	1.11
MPI-ESM-LR	0.35	1.38	0.49
MPI-ESM-MR	0.38	1.37	0.52
MPI-ESM-P	0.36	1.54	0.56
MRI-CGCM3	0.51	1.35	0.68
MRI-ESM1	0.51	1.31	0.67
NorESM1-M	0.83	1.06	0.88
bcc-csm1-1	0.88	0.62	0.55
bcc-csm1-1-m	0.90	0.89	0.80
inmcm4	0.95	1.13	1.08

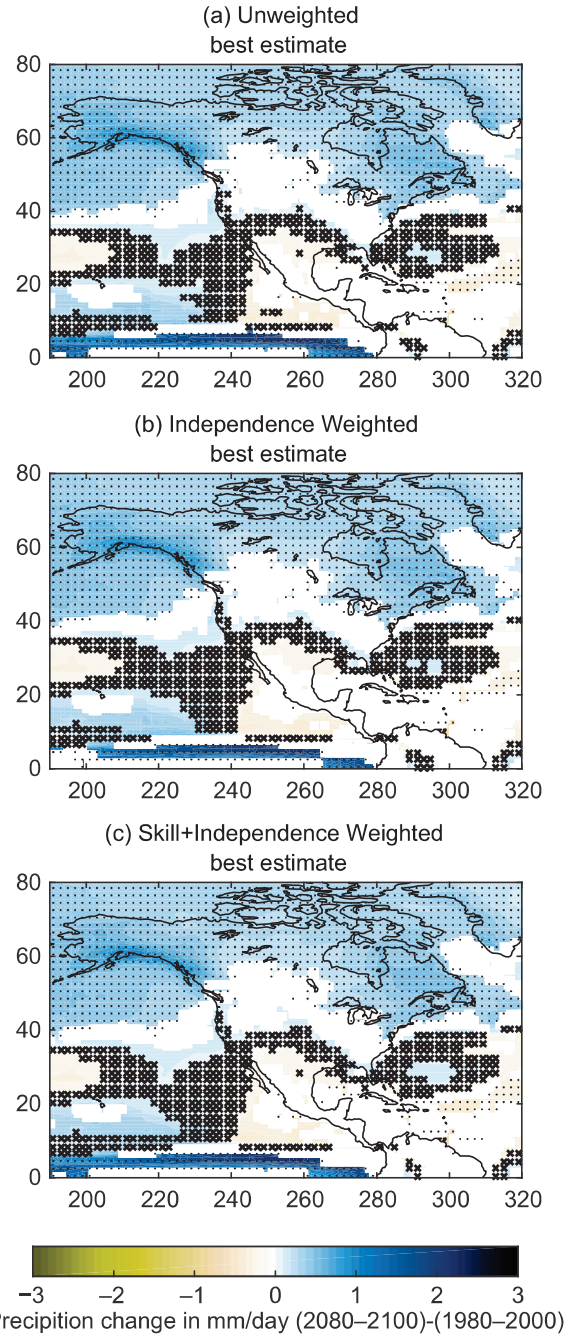

Figure B.3: Projections of precipitation change over North America in 2080–2100, relative to 1980–2000 under the higher scenario (RCP8.5). (a) Shows the simple unweighted CMIP5 multimodel average, using the significance methodology from IPCC[9]; (b) shows the weighted results as outlined in Section 3 for models weighted by uniqueness only; and (c) shows weighted results for models weighted by both uniqueness and skill. (Figure source: Sanderson et al. 2017[2]).

REFERENCES

1. Sanderson, B.M., R. Knutti, and P. Caldwell, 2015: A representative democracy to reduce interdependency in a multimodel ensemble. *Journal of Climate*, **28**, 5171-5194. http://dx.doi.org/10.1175/jcli-d-14-00362.1

2. Sanderson, B.M., M. Wehner, and R. Knutti, 2017: Skill and independence weighting for multi-model assessment. *Geoscientific Model Development*, **10**, 2379-2395. http://dx.doi.org/10.5194/gmd-10-2379-2017

3. Hopkinson, R.F., M.F. Hutchinson, D.W. McKenney, E.J. Milewska, and P. Papadopol, 2012: Optimizing input data for gridding climate normals for Canada. *Journal of Applied Meteorology and Climatology*, **51**, 1508-1518. http://dx.doi.org/10.1175/jamc-d-12-018.1

4. Hutchinson, M.F., D.W. McKenney, K. Lawrence, J.H. Pedlar, R.F. Hopkinson, E. Milewska, and P. Papadopol, 2009: Development and testing of Canada-wide interpolated spatial models of daily minimum–maximum temperature and precipitation for 1961–2003. *Journal of Applied Meteorology and Climatology*, **48**, 725-741. http://dx.doi.org/10.1175/2008jamc1979.1

5. Livneh, B., E.A. Rosenberg, C. Lin, B. Nijssen, V. Mishra, K.M. Andreadis, E.P. Maurer, and D.P. Lettenmaier, 2013: A long-term hydrologically based dataset of land surface fluxes and states for the conterminous United States: Update and extensions. *Journal of Climate*, **26**, 9384-9392. http://dx.doi.org/10.1175/jcli-d-12-00508.1

6. Wielicki, B.A., B.R. Barkstrom, E.F. Harrison, R.B. Lee III, G.L. Smith, and J.E. Cooper, 1996: Clouds and the Earth's Radiant Energy System (CERES): An Earth observing system experiment. *Bulletin of the American Meteorological Society*, **77**, 853-868. http://dx.doi.org/10.1175/1520-0477(1996)077<0853:catere>2.0.co;2

7. Aumann, H.H., M.T. Chahine, C. Gautier, M.D. Goldberg, E. Kalnay, L.M. McMillin, H. Revercomb, P.W. Rosenkranz, W.L. Smith, D.H. Staelin, L.L. Strow, and J. Susskind, 2003: AIRS/AMSU/HSB on the Aqua mission: Design, science objectives, data products, and processing systems. *IEEE Transactions on Geoscience and Remote Sensing*, **41**, 253-264. http://dx.doi.org/10.1109/tgrs.2002.808356

8. Uppala, S.M., P.W. KÅllberg, A.J. Simmons, U. Andrae, V.D.C. Bechtold, M. Fiorino, J.K. Gibson, J. Haseler, A. Hernandez, G.A. Kelly, X. Li, K. Onogi, S. Saarinen, N. Sokka, R.P. Allan, E. Andersson, K. Arpe, M.A. Balmaseda, A.C.M. Beljaars, L.V.D. Berg, J. Bidlot, N. Bormann, S. Caires, F. Chevallier, A. Dethof, M. Dragosavac, M. Fisher, M. Fuentes, S. Hagemann, E. Hólm, B.J. Hoskins, L. Isaksen, P.A.E.M. Janssen, R. Jenne, A.P. McNally, J.F. Mahfouf, J.J. Morcrette, N.A. Rayner, R.W. Saunders, P. Simon, A. Sterl, K.E. Trenberth, A. Untch, D. Vasiljevic, P. Viterbo, and J. Woollen, 2005: The ERA-40 re-analysis. *Quarterly Journal of the Royal Meteorological Society*, **131**, 2961-3012. http://dx.doi.org/10.1256/qj.04.176

9. IPCC, 2013: *Climate Change 2013: The Physical Science Basis. Contribution of Working Group I to the Fifth Assessment Report of the Intergovernmental Panel on Climate Change*. Cambridge University Press, Cambridge, UK and New York, NY, 1535 pp. http://www.climatechange2013.org/report/

Appendix C
Detection and Attribution Methodologies Overview

Recommended Citation for Chapter

Knutson, T., 2017: Detection and attribution methodologies overview. In: *Climate Science Special Report: Fourth National Climate Assessment, Volume I* [Wuebbles, D.J., D.W. Fahey, K.A. Hibbard, D.J. Dokken, B.C. Stewart, and T.K. Maycock (eds.)]. U.S. Global Change Research Program, Washington, DC, USA, pp. 443-451, doi: 10.7930/J0319T2J.

C.1 Introduction and Conceptual Framework

In this appendix, we present a brief overview of the methodologies and methodological issues for detection and attribution of climate change. Attributing an observed change or an event partly to a causal factor (such as anthropogenic climate forcing) normally requires that the change first be detectable.[1] A *detectable* observed change is one which is determined to be highly unlikely to occur (less than about a 10% chance) due to internal variability alone, without necessarily being ascribed to a causal factor. An *attributable* change refers to a change in which the relative contribution of causal factors has been evaluated along with an assignment of statistical confidence (e.g., Bindoff et al. 2013;[2] Hegerl et al. 2010[1]).

As outlined in Bindoff et al.,[2] the conceptual framework for most detection and attribution studies consists of four elements: 1) relevant observations; 2) the estimated time history of relevant climate forcings (such as greenhouse gas concentrations or volcanic activity); 3) a modeled estimate of the impact of the climate forcings on the climate variables of interest; and 4) an estimate of the internal (unforced) variability of the climate variables of interest—that is, the changes that can occur due to natural unforced variations of the ocean, atmosphere, land, cryosphere, and other elements of the climate system in the absence of external forcings. The four elements above can be used together with a detection and attribution framework to assess possible causes of observed changes.

C.2 Fingerprint-Based Methods

A key methodological approach for detection and attribution is the regression-based "fingerprint" method (e.g., Hasselmann 1997;[3] Allen and Stott 2003;[4] Hegerl et al. 2007;[5] Hegerl and Zwiers 2011;[6] Bindoff et al. 2013[2]), where observed changes are regressed onto a model-generated response pattern to a particular forcing (or set of forcings), and regression scaling factors are obtained. When a scaling factor for a forcing pattern is determined to be significantly different from zero, a detectable change has been identified. If the uncertainty bars on the scaling factor encompass unity, the observed change is consistent with the modeled response, and the observed change can be attributed, at least in part, to the associated forcing agent, according to this methodology. Zwiers et al.[7] showed how detection and attribution methods could be applied

to the problem of changes in daily temperature extremes at the regional scale by using a generalized extreme value (GEV) approach. In their approach, a time-evolving pattern of GEV location parameters (i.e., "fingerprint") from models is fit to the observed extremes as a means of detecting and attributing changes in the extremes to certain forcing sets (for example, anthropogenic forcings).

A recent development in detection/attribution methodology[8] uses hypothesis testing and an additive decomposition approach rather than linear regression of patterns. The new approach makes use of the magnitudes of responses from the models rather than using the model patterns and deriving the scaling factors (magnitudes of responses) from regression. The new method, in a first application, gives very similar attributable anthropogenic warming estimates to the earlier methods as reported in Bindoff et al.[2] and shown in Figure 3.2. Some further methodological developments for performing optimal fingerprint detection and attribution studies are proposed in Hannart,[9] who, for example, focuses on the possible use of raw data in analyses without the use of dimensional reductions, such as projecting the data onto a limited number of basis functions, such as spherical harmonics, before analysis.

C.3 Non-Fingerprint Based Methods

A simpler detection/attribution/consistency calculation, which does not involve regression and pattern scaling, compares observed and simulated time series to assess whether observations are consistent with natural variability simulations or with simulations forced by both natural and anthropogenic forcing agents.[10, 11] Cases where observations are inconsistent with model simulations using natural forcing only (a detectable change), while also being consistent with models that incorporate both anthropogenic and natural forcings, are interpreted as having an attributable anthropogenic contribution, subject to caveats regarding uncertainties in observations, climate forcings, modeled responses, and simulated internal climate variability. This simpler method is useful for assessing trends over smaller regions such as sub-regions of the United States (see the example given in Figure 6.5 for regional surface temperature trends).

Delsole et al.[12] introduced a method of identifying internal (unforced) variability in climate data by decomposing variables by time scale, using a measure of their predictability. They found that while such internal variability could contribute to surface temperature trends of 30-years' duration or less, and could be responsible for the accelerated global warming during 1977–2008 compared to earlier decades, the strong (approximately 0.8°C, or 1.4°F) warming trend seen in observations over the past century was not explainable by such internal variability. Constructed circulation analogs[13, 14] is a method used to identify the part of observed surface temperature changes that is due to atmospheric circulation changes alone.

The time scale by which climate change signals will become detectable in various regions is a question of interest in detection and attribution studies, and methods of estimating this have been developed and applied (e.g., Mahlstein et al. 2011;[15] Deser et al. 2012[16]). These studies illustrate how natural variability can obscure forced climate signals for decades, particularly for smaller (less than continental) space scales.

Other examples of detection and attribution methods include the use of multiple linear regression with energy balance models (e.g., Canty et al. 2013[17]) and Granger causality tests (e.g., Stern and Kaufmann 2014[18]). These are typically attempting to relate forcing time

series, such as the historical record of atmospheric CO_2 since 1860, to a climate response measure, such as global mean temperature or ocean heat content, but without using a full coupled climate model to explicitly estimate the response of the climate system to forcing (or the spatial pattern of the response to forcing). Granger causality, for example, explores the lead–lag relationships between different variables to infer causal relationships between them and attempts to control for any influence of a third variable that may be linked to the other two variables in question.

C.4 Multistep Attribution and Attribution without Detection

A growing number of climate change and extreme event attribution studies use a *multistep attribution* approach,[1] based on attribution of a change in climate conditions that are closely related to the variable or event of interest. In the multistep approach, an observed change in the variable of interest is attributed to a change in climate or other environmental conditions, and then the changes in the climate or environmental conditions are separately attributed to an external forcing, such as anthropogenic emissions of greenhouse gases. As an example, some attribution statements for phenomena such as droughts or hurricane activity—where there are not necessarily detectable trends in occurrence of the phenomenon itself—are based on models and on detected changes in related variables such as surface temperature, as well as an understanding of the relevant physical processes linking surface temperatures to hurricanes or drought. For example, some studies of the recent California drought (e.g., Mao et al. 2015;[19] Williams et al. 2015[20]) attribute a fraction of the event to anthropogenic warming or to long-term warming based on modeling or statistical analysis, although without claiming that there was a detectable change in the drought frequency or magnitude.

The multistep approach and model simulations are both methods that, in principle, can allow for attribution of a climate change or a change in the likelihood of occurrence of an event to a causal factor without necessarily detecting a significant change in the occurrence rate of the phenomenon or event itself (though in some cases, there may also be a detectable change in the variable of interest). For example, Murakami et al.[21] used model simulations to conclude that the very active hurricane season observed near Hawai'i in 2014 was at least partially attributable to anthropogenic influence; they also show that there is no clear long-term detectable trend in historical hurricane occurrence near Hawai'i in available observations. If an attribution statement is made where there is not a detectable change in the phenomenon itself (for example, hurricane frequency or drought frequency) then this statement is an example of *attribution without detection*. Such an attribution without detection can be distinguished from a conventional single-step attribution (for example, global mean surface temperature) where in the latter case there is a detectable change in the variable of interest (or the scaling factor for a forcing pattern is significantly different from zero in observations) and attribution of the changes in that variable to specific external forcing agents. Regardless of whether a single-step or multistep attribution approach is used, or whether there is a detectable change in the variable of interest, attribution statements with relatively higher levels of confidence are underpinned by a thorough understanding of the physical processes involved.

There are reasons why attribution without detection statements can be appropriate, despite the lower confidence typically associated with such statements as compared to attribution statements that are supported by detection of a change in the phenomenon itself. For example, an event of interest may be

so rare that a trend analysis for similar events is not practical. Including attribution without detection events in the analysis of climate change impacts reduces the chances of a false negative, that is, incorrectly concluding that climate change had no influence on a given extreme events[22] in a case where it did have an influence. However, avoiding this type of error through attribution without detection comes at the risk of increasing the rate of false positives, where one incorrectly concludes that anthropogenic climate change had a certain type of influence on an extreme event when in fact it did not have such an influence (see Box C.1).

C.5 Extreme Event Attribution Methodologies

Since the release of the Intergovernmental Panel on Climate Change's Fifth Assessment Report (IPCC AR5) and the Third National Climate Assessment (NCA3),[23] there have been further advances in the science of detection and attribution of climate change. An emerging area in the science of detection and attribution is the attribution of extreme weather and climate events.[24, 25, 26] According to Hulme,[27] there are four general types of attribution methods that are applied in practice: physical reasoning, statistical analysis of time series, fraction of attributable risk (FAR) estimation, and the philosophical argument that there are no longer any purely natural weather events. As discussed in a recent National Academy of Sciences report,[24] possible anthropogenic influence on an extreme event can be assessed using a risk-based approach, which examines whether the odds of occurrence of a type of extreme event have changed, or through an ingredients-based or conditional attribution approach.

In the risk-based approach,[24, 27, 28] one typically uses a model to estimate the probability (p) of occurrence of a weather or climate event within two climate states: one state with anthropogenic influence (where the probability is p_1) and the other state without anthropogenic influence (where the probability is p_0). Then the ratio (p_1 / p_0) describes how much more or less likely the event is in the modeled climate with anthropogenic influence compared to a modeled hypothetical climate without anthropogenic influences. Another common metric used with this approach is the fraction of attributable risk (FAR), defined as FAR = $1 - (p_0 / p_1)$. Further refinements on such an approach using causal theory are discussed in Hannart et al. [29]

In the conditional or ingredients-based approach,[24, 30, 31, 32] an investigator may look for changes in occurrence of atmospheric circulation and weather patterns relevant to the extreme event, or at the impact of certain environmental changes (for example, greater atmospheric moisture) on the character of an extreme event. Conditional or ingredients-based attribution can be applied to extreme events or to climate changes in general. An example of the ingredients-based approach and more discussion of this type of attribution method is given in Box C.2.

Hannart et al.[29] have discussed how causal theory can also be applied to attribution studies in order to distinguish between necessary and sufficient causation. Hannart et al.[33] further propose methodologies to use data assimilation systems, which are now used operationally to update short-term numerical weather prediction models, for detection and attribution. They envision how such systems could be used in the future to implement near-real time systematic causal attribution of weather and climate-related events.

Box C.1. On the Use of Significance Levels and Significance Tests in Attribution Studies

In detection/attribution studies, a detectable observed change is one which is determined to be highly unlikely to occur (less than about a 10% chance) due to internal variability alone. Some frequently asked questions concern the use of such a high statistical threshold (significance level) in attribution studies. In this box, we respond to several such questions received in the public review period.

Why is such a high degree of confidence (for example, statistical significance at p level of 0.05) typically required before concluding that an attributable anthropogenic component to a climate change or event has been detected? For example, could attribution studies be reframed to ask whether there is a 5% or more chance that anthropogenic climate change contributed to the event?

This question is partly related to the issue of risk avoidance. For example, if there is a particular climate change outcome that we wish to avoid (for example, global warming of 3°C, or 10°C, or a runaway greenhouse) then one can use the upper ranges of confidence intervals of climate model projections as guidance, based on available science, for avoiding such outcomes. Detection/attribution studies typically deal with smaller changes than climate projections over the next century or more. For detection/attribution studies, researchers are confronting models with historical data to explore whether or not observed climate change signals are emerging from the background of natural variability. Typically, the emergent signal is just a small fraction of what is predicted by the models for the coming century under continued strong greenhouse gas emission scenarios. Detecting that a change has emerged from natural variability is not the same as approaching a threshold to be avoided, unless the goal is to ensure no detectable anthropogenic influence on climate. Consequently, use of a relative strong confidence level (or *p*-value of 0.05) for determining climate change detection seems justified for the particular case of climate change detection, since one can also separately use risk-avoidance strategies or probability criteria to avoid reaching certain defined thresholds (for example, a 2°C global warming threshold).

A related question concerns ascribing blame for causing an extreme event. For example, if a damaging hurricane or typhoon strikes an area and causes much damage, affected residents may ask whether human-caused climate change was at least partially to blame for the event. In this case, climate scientists sometimes use the "Fraction of Attributable Risk" framework, where they examine whether the odds of some threshold event occurring have been increased due to anthropogenic climate change. This is typically a model-based calculation, where the probability distribution related to the event in question is modeled under preindustrial and present-day climate conditions, and the occurrence rates are compared for the two modeled distributions. Note that such an analysis can be done with or without the detection of a climate change signal for the occurrence of the event in question. In general, cases where there has been a detection and attribution of changes in the event in question to human causes, then the attribution of increased risk to anthropogenic forcing will be relatively more confident.

The question of whether it is more appropriate to use approaches that incorporate a high burden of statistical evidence before concluding that anthropogenic forcings contributed significantly (as in traditional detection/attribution studies) versus using models to estimate anthropogenic contributions when there may not even be a detectable signal present in the observations (as in some Fraction of Attributable Risk studies) may depend on what type of error or scenario one most wants to avoid. In the former case, one is attempting to avoid the error of concluding that anthropogenic forcing has contributed to some observed climate change, when in fact, it later turns out that anthropogenic forcing has not contributed to the change. In the second case, one is attempting to avoid the "error" of concluding that anthropogenic forcing has not contributed significantly to an observed

climate change or event when (as it later comes to be known) anthropogenic forcing had evidently contributed to the change, just not at a level that was detectable at the time compared to natural variability.

What is the tradeoff between false positives and false negatives in attribution statistical testing, and how is it decided which type of error one should focus on avoiding?

As discussed above, there are different types of errors or scenarios that we would ideally like to avoid. However, the decision of what type of analysis to do may involve a tradeoff where one decides that it is more important to avoid either falsely concluding that anthropogenic forcing *has* contributed, or to avoid falsely concluding that anthropogenic forcing had *not* made a detectable contribution to the event. Since there is no correct answer that can apply in all cases, it would be helpful if, in requesting scientific assessments, policymakers provide some guidance about which type of error or scenario they would most desire be avoided in the analyses and assessments in question.

Since substantial anthropogenic climate change (increased surface temperatures, increased atmospheric water vapor, etc.) has already occurred, aren't all extreme events affected to some degree by anthropogenic climate change?

Climate scientists are aware from modeling experiments that very tiny changes to initial conditions in model simulations lead to very different realizations of internal climate variability "noise" in the model simulations. Comparing large samples of this random background noise from models against observed changes is one way to test whether the observed changes are statistically distinguishable from internal climate variability. In any case, this experience also teaches us that any anthropogenic influence on climate, no matter how tiny, has some effect on the future trajectory of climate variability, and thus could affect the timing and occurrence of extreme events. More meaningful questions are: 1) Has anthropogenic forcing produced a statistically significant change in the probability of occurrence of some class of extreme event? 2) Can we determine with confidence the net sign of influence of anthropogenic climate change on the frequency, intensity, etc., of a type of extreme event? 3) Can climate scientists quantify (with credible confidence intervals) the effect of climate change on the occurrence frequency, the intensity, or some other aspect of an observed extreme event?

Box C.2 Illustration of Ingredients-based Event Attribution: The Case of Hurricane Sandy

To illustrate some aspects of the conditional or ingredients-based attribution approach, the case of Hurricane Sandy can be considered. If one considers Hurricane Sandy's surge event, there is strong evidence that sea level rise, at least partly anthropogenic in origin (see Ch. 12: Sea Level Rise), made Sandy's surge event worse, all other factors being equal.[34] The related question of whether anthropogenic climate change increased the risk of an event like Sandy involves not just the sea level ingredient to surge risk but also whether the frequency and/or intensity of Sandy-like storms has increased or decreased as a result of anthropogenic climate change. This latter question is more difficult and is briefly reviewed here.

A conditional or ingredients-based attribution approach, as applied to a hurricane event such as Sandy, may assume that the weather patterns in which the storm was embedded—and the storm itself—could have occurred in a preindustrial climate, and the event is re-simulated while changing only some aspects of the large-scale environment (for example, sea surface temperatures, atmospheric temperatures, and moisture) by an estimated anthropogenic climate change signal. Such an approach thus explores whether anthropogenic climate change to date has, for example, altered the intensity of a Hurricane Sandy-like storm, assuming the occurrence of a Sandy-like storm in both preindustrial and present-day climates. Modeling studies show, as expected, that the anomalously warm sea surface temperatures off the U.S. East Coast during Sandy led to a substantially more intense simulated storm than under present-day climatological conditions.[35] However, these anomalous sea surface temperatures and other environmental changes are a mixture of anthropogenic and natural influences, and so it is not generally possible to infer the anthropogenic component from such experiments. Another study[36] modeled the influence of just the anthropogenic changes to the thermodynamic environment (including sea surface temperatures, atmospheric temperatures, and moisture perturbations) and concluded that anthropogenic climate change to date had caused Hurricane Sandy to be about 5 hPa more intense, but that this modeled change was not statistically significant at the 95% confidence level. A third study used a statistical–dynamical model to compare simulated New York City-area tropical cyclones in pre-anthropogenic and anthropogenic time periods.[34] It concluded that there have been anthropogenically induced increases in the types of tropical cyclones that cause extreme surge events in the region, apart from the effects of sea level rise, such as increased radius of maximum winds in the anthropogenic era. However, the statistical–dynamical model used in the study simulates an unusually large increase in global tropical cyclone activity in 21st century projections[37] compared to other tropical cyclone modeling studies using dynamical models—a number of which simulate future decreases in late 21st century tropical storm frequency in the Atlantic basin (e.g., Christensen et al. 2013[38]). This range of uncertainty among various model simulations of Atlantic tropical cyclone activity under climate change imply that there is low confidence in determining the net impact to date of anthropogenic climate change on the risk of Sandy-like events, though anthropogenic sea level rise, all other things equal, has increased the surge risk.

In summary, while there is agreement that sea level rise alone has caused greater storm surge risk in the New York City area, there is low confidence on whether a number of other important determinants of storm surge climate risk, such as the frequency, size, or intensity of Sandy-like storms in the New York region, have increased or decreased due to anthropogenic warming to date.

REFERENCES

1. Hegerl, G.C., O. Hoegh-Guldberg, G. Casassa, M.P. Hoerling, R.S. Kovats, C. Parmesan, D.W. Pierce, and P.A. Stott, 2010: Good practice guidance paper on detection and attribution related to anthropogenic climate change. *Meeting Report of the Intergovernmental Panel on Climate Change Expert Meeting on Detection and Attribution of Anthropogenic Climate Change*. Stocker, T.F., C.B. Field, D. Qin, V. Barros, G.-K. Plattner, M. Tignor, P.M. Midgley, and K.L. Ebi, Eds. IPCC Working Group I Technical Support Unit, University of Bern, Bern, Switzerland, 1-8. http://www.ipcc.ch/pdf/supporting-material/ipcc_good_practice_guidance_paper_anthropogenic.pdf

2. Bindoff, N.L., P.A. Stott, K.M. AchutaRao, M.R. Allen, N. Gillett, D. Gutzler, K. Hansingo, G. Hegerl, Y. Hu, S. Jain, I.I. Mokhov, J. Overland, J. Perlwitz, R. Sebbari, and X. Zhang, 2013: Detection and attribution of climate change: From global to regional. *Climate Change 2013: The Physical Science Basis. Contribution of Working Group I to the Fifth Assessment Report of the Intergovernmental Panel on Climate Change*. Stocker, T.F., D. Qin, G.-K. Plattner, M. Tignor, S.K. Allen, J. Boschung, A. Nauels, Y. Xia, V. Bex, and P.M. Midgley, Eds. Cambridge University Press, Cambridge, United Kingdom and New York, NY, USA, 867–952. http://www.climatechange2013.org/report/full-report/

3. Hasselmann, K., 1997: Multi-pattern fingerprint method for detection and attribution of climate change. *Climate Dynamics*, **13**, 601-611. http://dx.doi.org/10.1007/s003820050185

4. Allen, M.R. and P.A. Stott, 2003: Estimating signal amplitudes in optimal fingerprinting, Part I: Theory. *Climate Dynamics*, **21**, 477-491. http://dx.doi.org/10.1007/s00382-003-0313-9

5. Hegerl, G.C., F.W. Zwiers, P. Braconnot, N.P. Gillett, Y. Luo, J.A.M. Orsini, N. Nicholls, J.E. Penner, and P.A. Stott, 2007: Understanding and attributing climate change. *Climate Change 2007: The Physical Science Basis. Contribution of Working Group I to the Fourth Assessment Report of the Intergovernmental Panel on Climate Change*. Solomon, S., D. Qin, M. Manning, Z. Chen, M. Marquis, K.B. Averyt, M. Tignor, and H.L. Miller, Eds. Cambridge University Press, Cambridge, United Kingdom and New York, NY, USA, 663-745. http://www.ipcc.ch/publications_and_data/ar4/wg1/en/ch9.html

6. Hegerl, G. and F. Zwiers, 2011: Use of models in detection and attribution of climate change. *Wiley Interdisciplinary Reviews: Climate Change*, **2**, 570-591. http://dx.doi.org/10.1002/wcc.121

7. Zwiers, F.W., X.B. Zhang, and Y. Feng, 2011: Anthropogenic influence on long return period daily temperature extremes at regional scales. *Journal of Climate*, **24**, 881-892. http://dx.doi.org/10.1175/2010jcli3908.1

8. Ribes, A., F.W. Zwiers, J.-M. Azaïs, and P. Naveau, 2017: A new statistical approach to climate change detection and attribution. *Climate Dynamics*, **48**, 367-386. http://dx.doi.org/10.1007/s00382-016-3079-6

9. Hannart, A., 2016: Integrated optimal fingerprinting: Method description and illustration. *Journal of Climate*, **29**, 1977-1998. http://dx.doi.org/10.1175/jcli-d-14-00124.1

10. Knutson, T.R., F. Zeng, and A.T. Wittenberg, 2013: Multimodel assessment of regional surface temperature trends: CMIP3 and CMIP5 twentieth-century simulations. *Journal of Climate*, **26**, 8709-8743. http://dx.doi.org/10.1175/JCLI-D-12-00567.1

11. van Oldenborgh, G.J., F.J. Doblas Reyes, S.S. Drijfhout, and E. Hawkins, 2013: Reliability of regional climate model trends. *Environmental Research Letters*, **8**, 014055. http://dx.doi.org/10.1088/1748-9326/8/1/014055

12. DelSole, T., M.K. Tippett, and J. Shukla, 2011: A significant component of unforced multidecadal variability in the recent acceleration of global warming. *Journal of Climate*, **24**, 909-926. http://dx.doi.org/10.1175/2010jcli3659.1

13. van den Dool, H., J. Huang, and Y. Fan, 2003: Performance and analysis of the constructed analogue method applied to U.S. soil moisture over 1981–2001. *Journal of Geophysical Research*, **108**, 8617. http://dx.doi.org/10.1029/2002JD003114

14. Deser, C., L. Terray, and A.S. Phillips, 2016: Forced and internal components of winter air temperature trends over North America during the past 50 years: Mechanisms and implications. *Journal of Climate*, **29**, 2237-2258. http://dx.doi.org/10.1175/JCLI-D-15-0304.1

15. Mahlstein, I., R. Knutti, S. Solomon, and R.W. Portmann, 2011: Early onset of significant local warming in low latitude countries. *Environmental Research Letters*, **6**, 034009. http://dx.doi.org/10.1088/1748-9326/6/3/034009

16. Deser, C., R. Knutti, S. Solomon, and A.S. Phillips, 2012: Communication of the role of natural variability in future North American climate. *Nature Climate Change*, **2**, 775-779. http://dx.doi.org/10.1038/nclimate1562

17. Canty, T., N.R. Mascioli, M.D. Smarte, and R.J. Salawitch, 2013: An empirical model of global climate – Part 1: A critical evaluation of volcanic cooling. *Atmospheric Chemistry and Physics*, **13**, 3997-4031. http://dx.doi.org/10.5194/acp-13-3997-2013

18. Stern, D.I. and R.K. Kaufmann, 2014: Anthropogenic and natural causes of climate change. *Climatic Change*, **122**, 257-269. http://dx.doi.org/10.1007/s10584-013-1007-x

19. Mao, Y., B. Nijssen, and D.P. Lettenmaier, 2015: Is climate change implicated in the 2013–2014 California drought? A hydrologic perspective. *Geophysical Research Letters*, **42**, 2805-2813. http://dx.doi.org/10.1002/2015GL063456

20. Williams, A.P., R. Seager, J.T. Abatzoglou, B.I. Cook, J.E. Smerdon, and E.R. Cook, 2015: Contribution of anthropogenic warming to California drought during 2012–2014. *Geophysical Research Letters*, **42**, 6819-6828. http://dx.doi.org/10.1002/2015GL064924

21. Murakami, H., G.A. Vecchi, T.L. Delworth, K. Paffendorf, L. Jia, R. Gudgel, and F. Zeng, 2015: Investigating the influence of anthropogenic forcing and natural variability on the 2014 Hawaiian hurricane season [in "Explaining Extreme Events of 2014 from a Climate Perspective"]. *Bulletin of the American Meteorological Society*, **96 (12)**, S115-S119. http://dx.doi.org/10.1175/BAMS-D-15-00119.1

22. Anderegg, W.R.L., E.S. Callaway, M.T. Boykoff, G. Yohe, and T.y.L. Root, 2014: Awareness of both type 1 and 2 errors in climate science and assessment. *Bulletin of the American Meteorological Society*, **95**, 1445-1451. http://dx.doi.org/10.1175/BAMS-D-13-00115.1

23. Melillo, J.M., T.C. Richmond, and G.W. Yohe, eds., 2014: *Climate Change Impacts in the United States: The Third National Climate Assessment*. U.S. Global Change Research Program: Washington, D.C., 841 pp. http://dx.doi.org/10.7930/J0Z31WJ2

24. NAS, 2016: *Attribution of Extreme Weather Events in the Context of Climate Change*. The National Academies Press, Washington, DC, 186 pp. http://dx.doi.org/10.17226/21852

25. Stott, P., 2016: How climate change affects extreme weather events. *Science*, **352**, 1517-1518. http://dx.doi.org/10.1126/science.aaf7271

26. Easterling, D.R., K.E. Kunkel, M.F. Wehner, and L. Sun, 2016: Detection and attribution of climate extremes in the observed record. *Weather and Climate Extremes*, **11**, 17-27. http://dx.doi.org/10.1016/j.wace.2016.01.001

27. Hulme, M., 2014: Attributing weather extremes to 'climate change'. *Progress in Physical Geography*, **38**, 499-511. http://dx.doi.org/10.1177/0309133314538644

28. Stott, P.A., D.A. Stone, and M.R. Allen, 2004: Human contribution to the European heatwave of 2003. *Nature*, **432**, 610-614. http://dx.doi.org/10.1038/nature03089

29. Hannart, A., J. Pearl, F.E.L. Otto, P. Naveau, and M. Ghil, 2016: Causal counterfactual theory for the attribution of weather and climate-related events. *Bulletin of the American Meteorological Society*, **97**, 99-110. http://dx.doi.org/10.1175/bams-d-14-00034.1

30. Horton, R.M., J.S. Mankin, C. Lesk, E. Coffel, and C. Raymond, 2016: A review of recent advances in research on extreme heat events. *Current Climate Change Reports*, **2**, 242-259. http://dx.doi.org/10.1007/s40641-016-0042-x

31. Shepherd, T.G., 2016: A common framework for approaches to extreme event attribution. *Current Climate Change Reports*, **2**, 28-38. http://dx.doi.org/10.1007/s40641-016-0033-y

32. Trenberth, K.E., J.T. Fasullo, and T.G. Shepherd, 2015: Attribution of climate extreme events. *Nature Climate Change*, **5**, 725-730. http://dx.doi.org/10.1038/nclimate2657

33. Hannart, A., A. Carrassi, M. Bocquet, M. Ghil, P. Naveau, M. Pulido, J. Ruiz, and P. Tandeo, 2016: DADA: Data assimilation for the detection and attribution of weather and climate-related events. *Climatic Change*, **136**, 155-174. http://dx.doi.org/10.1007/s10584-016-1595-3

34. Reed, A.J., M.E. Mann, K.A. Emanuel, N. Lin, B.P. Horton, A.C. Kemp, and J.P. Donnelly, 2015: Increased threat of tropical cyclones and coastal flooding to New York City during the anthropogenic era. *Proceedings of the National Academy of Sciences*, **112**, 12610-12615. http://dx.doi.org/10.1073/pnas.1513127112

35. Magnusson, L., J.-R. Bidlot, S.T.K. Lang, A. Thorpe, N. Wedi, and M. Yamaguchi, 2014: Evaluation of medium-range forecasts for Hurricane Sandy. *Monthly Weather Review*, **142**, 1962-1981. http://dx.doi.org/10.1175/mwr-d-13-00228.1

36. Lackmann, G.M., 2015: Hurricane Sandy before 1900 and after 2100. *Bulletin of the American Meteorological Society*, **96 (12)**, 547-560. http://dx.doi.org/10.1175/BAMS-D-14-00123.1

37. Emanuel, K.A., 2013: Downscaling CMIP5 climate models shows increased tropical cyclone activity over the 21st century. *Proceedings of the National Academy of Sciences*, **110**, 12219-12224. http://dx.doi.org/10.1073/pnas.1301293110

38. Christensen, J.H., K. Krishna Kumar, E. Aldrian, S.-I. An, I.F.A. Cavalcanti, M. de Castro, W. Dong, P. Goswami, A. Hall, J.K. Kanyanga, A. Kitoh, J. Kossin, N.-C. Lau, J. Renwick, D.B. Stephenson, S.-P. Xie, and T. Zhou, 2013: Climate phenomena and their relevance for future regional climate change. *Climate Change 2013: The Physical Science Basis. Contribution of Working Group I to the Fifth Assessment Report of the Intergovernmental Panel on Climate Change*. Stocker, T.F., D. Qin, G.-K. Plattner, M. Tignor, S.K. Allen, J. Boschung, A. Nauels, Y. Xia, V. Bex, and P.M. Midgley, Eds. Cambridge University Press, Cambridge, United Kingdom and New York, NY, USA, 1217–1308. http://www.climatechange2013.org/report/full-report/

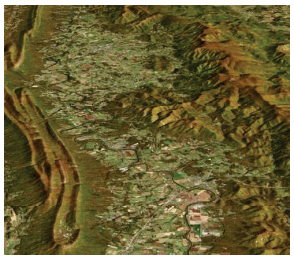

Appendix D
Acronyms and Units

doi: 10.7930/J0ZC811D

AGCM	atmospheric general circulation model
AIS	Antarctic Ice Sheet
AMO	Atlantic Multidecadal Oscillation
AMOC	Atlantic meridional overturning circulation
AMSU	Advanced Microwave Sounding Unit
AO	Arctic Oscillation
AOD	aerosol optical depth
AR	atmospheric river
AW	Atlantic Water
BAMS	Bulletin of the American Meteorological Society
BC	black carbon
BCE	Before Common Era
CAM5	Community Atmospheric Model, Version 5
CAPE	convective available potential energy
CCN	cloud condensation nuclei
CCSM3	Community Climate System Model, Version 3
CDR	carbon dioxide removal
CE	Common Era
CENRS	Committee on Environment, Natural Resources, and Sustainability (National Science and Technology Council, White House)

CESM-LE	Community Earth System Model Large Ensemble Project
CFCs	chlorofluorocarbons
CI	climate intervention
CMIP5	Coupled Model Intercomparison Project, Fifth Phase (also CMIP3 and CMIP6)
CONUS	contiguous United States
CP	Central Pacific
CSSR	Climate Science Special Report
DIC	dissolved inorganic carbon
DJF	December-January-February
DoD SERDP	U.S. Department of Defense, Strategic Environmental Research and Development Program
DOE	U.S. Department of Energy
EAIS	East Antarctic Ice Sheet
ECS	equilibrium climate sensitivity
ENSO	El Niño–Southern Oscillation
EOF analysis	empirical orthogonal function analysis
EP	Eastern Pacific
ERF	effective radiative forcing
ESD	empirical statistical downscaling
ESDM	empirical statistical downscaling model
ESM	Earth System Model
ESS	Earth system sensitivity
ETC	extratropical cyclone
ETCCDI	Expert Team on Climate Change Detection Indices
GBI	Greenland Blocking Index

GCIS	Global Change Information System
GCM	global climate model
GeoMIP	Geoengineering Model Intercomparison Project
GFDL HiRAM	Geophysical Fluid Dynamics Laboratory, global HIgh Resolution Atmospheric Model (NOAA)
GHCN	Global Historical Climatology Network (National Centers for Environmental Information, NOAA)
GHG	greenhouse gas
GMSL	global mean sea level
GMT	global mean temperature
GPS	global positioning system
GRACE	Gravity Recovery and Climate Experiment
GrIS	Greenland Ice Sheet
GWP	global warming potential
HadCM3	Hadley Centre Coupled Model, Version 3
HadCRUT4	Hadley Centre Climatic Research Unit Gridded Surface Temperature Dataset 4
HCFCs	hydrochlorofluorocarbons
HFCs	hydrofluorocarbons
HOT	Hawai'i Ocean Time-series
HOT-DOGS	Hawai'i Ocean Time-series Data Organization & Graphical System
HURDAT2	revised Atlantic Hurricane Database (National Hurricane Center, NOAA)
IAM	integrated assessment model
IAV	impacts, adaptation, and vulnerability
INMCM	Institute for Numerical Mathematics Climate Model
IPCC	Intergovernmental Panel on Climate Change

IPCC AR5	Fifth Assessment Report of the IPCC; also SPM—Summary for Policymakers, and WG1, WG2, WG3—Working Groups 1–3
IPO	Interdecadal Pacific Oscillation
IVT	integrated vapor transport
JGOFS	U.S. Joint Global Ocean Flux Study
JJA	June-July-August
JTWC	Joint Typhoon Warning Center
LCC	land-cover changes
LULCC	land-use and land-cover change
MAM	March-April-May
MSU	Microwave Sounding Unit
NAM	Northern Annular Mode
NAO	North Atlantic Oscillation
NARCCAP	North American Regional Climate Change Assessment Program (World Meteorological Organization)
NAS	National Academy of Sciences
NASA	National Aeronautics and Space Administration
NCA	National Climate Assessment
NCA3	Third National Climate Assessment
NCA4	Fourth National Climate Assessment
NCEI	National Centers for Environmental Information (NOAA)
NDC	nationally determined contribution
NOAA	National Oceanic and Atmospheric Administration
NPI	North Pacific Index
NPO	North Pacific oscillation

NPP	net primary production
OMZs	oxygen minimum zones
OSTP	Office of Science and Technology Policy (White House)
PCA	principle component analysis
PDO	Pacific Decadal Oscillation
PDSI	Palmer Drought Severity Index
PETM	Paleo-Eocene Thermal Maximum
PFCs	perfluorocarbons
PGW	pseudo-global warming
PNA	Pacific North American Pattern
RCM	regional climate models
RCP	Representative Concentration Pathway
RF	radiative forcing
RFaci	aerosol–cloud interaction (effect on RF)
RFari	aerosol–radiation interaction (effect on RF)
RMSE	root mean square error
RSL	relative sea level
RSS	remote sensing systems
S06	surface-to-6 km layer
SCE	snow cover extent
SGCR	Subcommittee on Global Change Research (National Science and Technology Council, White House)
SLCF	short-lived climate forcer
SLCP	short-lived climate pollutant
SLR	sea level rise

SOC	soil organic carbon
SRES	IPCC Special Report on Emissions Scenarios
SREX	IPCC Special Report on Managing the Risks of Extreme Events and Disasters to Advance Climate Change Adaptation
SRM	solar radiation management
SSC	Science Steering Committee
SSI	solar spectral irradiance
SSP	Shared Socioeconomic Pathway
SST	sea surface temperature
STAR	Center for Satellite Applications and Research (NOAA)
SWCRE	shortwave cloud radiative effect (on radiative fluxes)
LWCRE	longwave cloud radiative effect (on radiative fluxes)
TA	total alkalinity
TC	tropical cyclone
TCR	transient climate response
TCRE	transient climate response to cumulative carbon emissions
TOPEX/JASON1,2	Topography Experiment/Joint Altimetry Satellite Oceanography Network satellites (NASA)
TSI	total solar irradiance
TTT	temperature total troposphere
UAH	University of Alabama, Huntsville
UHI	urban heat island (effect)
UNFCCC	United Nations Framework Convention on Climate Change
USGCRP	U.S. Global Change Research Program
USGS	U.S. Geological Survey

UV	ultraviolet
VOCs	volatile organic compounds
WAIS	West Antarctic Ice Sheet
WCRP	World Climate Research Programme
WMGHG	well-mixed greenhouse gas
WOCE	World Ocean Circulation Experiment (JGOFS)

Abbreviations and Units

C	carbon
CO	carbon monoxide
CH_4	methane
cm	centimeters
CO_2	carbon dioxide
°C	degrees Celsius
°F	degrees Fahrenheit
GtC	gigatonnes of carbon
hPA	hectopascal
H_2S	hydrogen sulfide
H_2SO_4	sulfuric acid
km	kilometers
m	meters
mm	millimeters
Mt	megaton
µatm	microatmosphere
N	nitrogen

N_2O	nitrous oxide
NO_x	nitrogen oxides
O_2	molecular oxygen
O_3	ozone
OH	hydroxyl radical
PgC	petagrams of carbon
ppb	parts per billion
ppm	parts per million
SF_6	sulfur hexafluoride
SO_2	sulfur dioxide
TgC	teragrams of carbon
W/m^2	Watts per meter squared

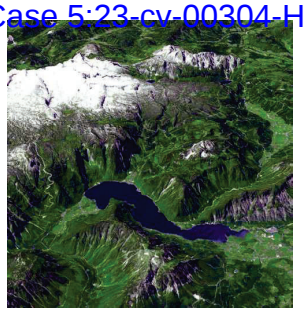

Appendix E
Glossary Terms

doi: 10.7930/J0TM789P

Abrupt climate change
Change in the climate system on a timescale shorter than the timescale of the responsible forcing. In the case of anthropogenic forcing over the past century, abrupt change occurs over decades or less. Abrupt change need not be externally forced. (*CSSR, Ch. 15*)

Aerosol–cloud interaction
A process by which a perturbation to aerosol affects the microphysical properties and evolution of clouds through the aerosol role as cloud condensation nuclei or ice nuclei, particularly in ways that affect radiation or precipitation; such processes can also include the effect of clouds and precipitation on aerosol. The aerosol perturbation can be anthropogenic or come from some natural source. The radiative forcing from such interactions has traditionally been attributed to numerous indirect aerosol effects, but in this report, only two levels of radiative forcing (or effect) are distinguished:

The radiative forcing (or effect) due to aerosol–cloud interactions (**RFaci**) is the radiative forcing (or radiative effect, if the perturbation is internally generated) due to the change in number or size distribution of cloud droplets or ice crystals that is the proximate result of an aerosol perturbation, with other variables (in particular total cloud water content) remaining equal. In liquid clouds, an increase in cloud droplet concentration and surface area would increase the cloud albedo. This effect is also known as the cloud albedo effect, first indirect effect, or Twomey effect. It is a largely theoretical concept that cannot readily be isolated in observations or comprehensive process models due to the rapidity and ubiquity of rapid adjustments. This is contrasted with the effective radiative forcing (or effect) due to aerosol–cloud interactions (ERFaci)

The total effective radiative forcing due to both aerosol–cloud and aerosol–radiation interactions is denoted aerosol effective radiative forcing (ERFari+aci). See also **aerosol–radiation interaction**. (condensed from IPCC AR5 WGI Annex III: Glossary)

Aerosol–radiation interaction (RFari)
The radiative forcing (or radiative effect, if the perturbation is internally generated) of an aerosol perturbation due directly to aerosol–radiation interactions, with all environmental variables remaining unaffected. It is traditionally known in the literature as the *direct aerosol forcing* (or *effect*).

The total effective radiative forcing due to both aerosol–cloud and aerosol–radiation interactions is denoted aerosol effective radiative forcing (ERFari+aci). See also **aerosol-cloud interaction**. (condensed from IPCC AR5 WGI Annex III: Glossary)

Agricultural drought
See **drought**.

Albedo
The fraction of solar radiation reflected by a surface or object, often expressed as a percentage. Snow-covered surfaces have a high albedo, the albedo of soils ranges from high to low, and vegetation-covered surfaces and oceans have a low albedo. The Earth's planetary albedo varies mainly through varying cloudiness, snow, ice, leaf area, and land-cover changes. (IPCC AR5 WGI Annex III: Glossary)

Altimetry
A technique for measuring the height of the Earth's surface with respect to the geocenter of the Earth within a defined terrestrial reference

frame (geocentric sea level). (IPCC AR5 WGI Annex III: Glossary)

Anticyclonic circulation
Fluid motion having a sense of rotation about the local vertical opposite to that of the earth's rotation; that is, clockwise in the Northern Hemisphere, counterclockwise in the Southern Hemisphere, and undefined at the equator. It is the opposite of **cyclonic circulation**. (AMS glossary).

Atlantic meridional overturning circulation (AMOC)
See **Meridional overturning circulation (MOC)**.

Atmospheric blocking
See **Blocking**.

Atmospheric river
A long, narrow, and transient corridor of strong horizontal water vapor transport that is typically associated with a low-level jet stream ahead of the cold front of an extratropical cyclone. The water vapor in atmospheric rivers is supplied by tropical and/or extratropical moisture sources. Atmospheric rivers frequently lead to heavy precipitation where they are forced upward—for example, by mountains or by ascent in the warm conveyor belt. Horizontal water vapor transport in the midlatitudes occurs primarily in atmospheric rivers and is focused in the lower troposphere. (AMS glossary).

Baroclinicity
The state of stratification in a fluid in which surfaces of constant pressure (isobaric) intersect surfaces of constant density (isosteric). (AMS glossary).

Bias correction method
One of two main statistical approaches used to alleviate the limitations of global and regional climate models, in which the statistics of the simulated model outputs are adjusted to those of the observation data. (The other approach is **empirical/stochastic downscaling**, described under **downscaling**). The rescaled variables can remove the effects of systematic errors in climate model outputs. (derived from Kim et al., 2015)

Biological pump
The suite of biologically mediated processes responsible for transporting carbon against a concentration gradient from the upper ocean to the deep ocean. (Passow and Carlson, 2012)

Blocking
Associated with persistent, slow-moving high pressure systems that obstruct the prevailing westerly winds in the middle and high latitudes and the normal eastward progress of extratropical transient storm systems. It is an important component of the intraseasonal climate variability in the extratropics and can cause long-lived weather conditions such as cold spells in winter and heat waves in summer. (IPCC AR5 WGI Annex III: Glossary)

Carbon dioxide fertilization
The enhancement of the growth of plants as a result of increased atmospheric CO_2 concentration. (IPCC AR5 WGI Annex III: Glossary)

Carbon dioxide removal
A set of techniques that aim to remove CO_2 directly from the atmosphere by either (1) increasing natural sinks for carbon or (2) using chemical engineering to remove the CO_2, with the intent of reducing the atmospheric CO_2 concentration. CDR methods involve the ocean, land and technical systems, including such methods as iron fertilization, large-scale afforestation and direct capture of CO_2 from the atmosphere using engineered chemical means. (truncated version from IPCC AR5 WGI Annex III: Glossary)

Climate engineering
See **geoengineering**.

Climate intervention
See **geoengineering**.

Climate sensitivity
In Intergovernmental Panel on Climate Change (IPCC) reports, **equilibrium climate sensitivity** (units: °C) refers to the equilibrium (steady state) change in the annual global mean surface temperature following a doubling of the atmospheric equivalent carbon dioxide concentration. The **effective climate sensitivity** (units: °C) is an estimate of the global mean surface temperature re-

sponse to doubled carbon dioxide concentration that is evaluated from model output or observations for evolving non-equilibrium conditions. It is a measure of the strengths of the climate feedbacks at a particular time and may vary with forcing history and climate state, and therefore may differ from equilibrium climate sensitivity. The **transient climate response** (units: °C) is the change in the global mean surface temperature, averaged over a 20-year period centered at the time of atmospheric carbon dioxide doubling, in a climate model simulation in which CO_2 increases at 1% per year. It is a measure of the strength and rapidity of the surface temperature response to greenhouse gas forcing. (IPCC AR5 WGI Annex III: Glossary)

Cloud radiative effect
The radiative effect of clouds relative to the identical situation without clouds (previously called cloud radiative forcing). (drawn from IPCC AR5 WGI Annex III: Glossary)

Clouds can act as a greenhouse ingredient to warm the Earth by trapping outgoing longwave infrared radiative flux at the top of the atmosphere (the **longwave cloud radiative effect [LWCRE]**). Clouds can also enhance the planetary albedo by reflecting shortwave solar radiative flux back to space to cool the Earth (the **shortwave cloud radiative effect [SWCRE]**). The net effect of the two competing processes depends on the height, type, and the optical properties of the clouds. (edited from *NOAA*, Geophysical Fluid Dynamics Laboratory)

CMIP
The Coupled Model Intercomparison Project is a standard experimental protocol for studying the output of coupled atmosphere–ocean general circulation models (AOGCMs). Phases three and five (CMIP3 and CMIP5, respectively) coordinated and archived climate model simulations based on shared model inputs by modeling groups from around the world. The CMIP3 multi-model data set includes projections using the SRES scenarios drawn from the Intergovernmental Panel on Climate Change's Special Report on Emissions Scenarios. The CMIP5 dataset includes projections using the **Representative Concentration Pathways**. (edited from IPCC AR5 WGII Annex II: Glossary).

Compound event
An event that consists of 1) two or more extreme events occurring simultaneously or successively, 2) combinations of extreme events with underlying conditions that amplify the impact of the events, or 3) combinations of events that are not themselves extremes but lead to an extreme event or impact when combined. The contributing events can be of similar or different types. (*CSSR, Ch. 15*, drawing upon *SREX 3.1.3*)

Critical threshold
A threshold that arises within a system as a result of the amplifying effects of positive **feedbacks**. The crossing of a critical threshold commits the system to a change in state. (*CSSR, Ch. 15*)

Cryosphere
All regions on and beneath the surface of the Earth and ocean where water is in solid form, including sea ice, lake ice, river ice, snow cover, glaciers and ice sheets, and frozen ground (which includes permafrost). (IPCC AR5 WGI Annex III: Glossary)

Cyclonic circulation
Fluid motion in the same sense as that of the earth, that is, counterclockwise in the Northern Hemisphere, clockwise in the Southern Hemisphere, undefined at the equator. (AMS glossary).

Denitrification
As used in this report, refers to the loss of fixed nitrogen in the ocean through biogeochemical processes. (*CSSR, Ch. 13*).

Deoxygenation
See **hypoxia**.

Downscaling
A method that derives local- to regional-scale (10–100 km) information from larger-scale models or data analyses. Two main methods exist. **Dynamical downscaling** uses the output of regional climate models, global models with variable spatial resolution, or high-resolution global models. **Empirical/statistical downscal-**

ing methods develop statistical relationships that link the large-scale atmospheric variables with local/regional climate variables. In all cases, the quality of the driving model remains an important limitation on the quality of the downscaled information. (IPCC AR5 WGI Annex III: Glossary)

Drought
A period of abnormally dry weather long enough to cause a serious hydrological imbalance. Drought is a relative term; therefore, any discussion in terms of precipitation deficit must refer to the particular precipitation-related activity that is under discussion. For example, shortage of precipitation during the growing season impinges on crop production or ecosystem function in general (due to soil moisture drought, also termed **agricultural drought**), and during the runoff and percolation season primarily affects water supplies (**hydrological drought**). Storage changes in soil moisture and groundwater are also affected by increases in actual evapotranspiration in addition to reductions in precipitation. A period with an abnormal precipitation deficit is defined as a **meteorological drought**. (IPCC AR5 WGI Annex III: Glossary)

Dynamical downscaling
See **downscaling**.

Earth System Model
A coupled atmosphere–ocean general circulation model in which a representation of the carbon cycle is included, allowing for interactive calculation of atmospheric CO_2 or compatible emissions. Additional components (for example, atmospheric chemistry, ice sheets, dynamic vegetation, nitrogen cycle, but also urban or crop models) may be included. (IPCC AR5 WGI Annex III: Glossary)

Effective radiative forcing
See **radiative forcing**.

El Niño–Southern Oscillation
A natural variability in ocean water surface pressure that causes periodic changes in ocean surface temperatures in the tropical Pacific Ocean. El Niño–Southern Oscillation (ENSO) has two phases: the warm oceanic phase, El Niño, accompanies high air surface pressure in the western Pacific, while the cold phase, La Niña, accompanies low air surface pressure in the western Pacific. Each phase generally lasts for 6 to 18 months. ENSO events occur irregularly, roughly every 3 to 7 years. The extremes of this climate pattern's oscillations cause extreme weather (such as floods and droughts) in many regions of the world. (*USGCRP*)

Empirical/statistical downscaling
See **downscaling**.

Equivalent carbon dioxide concentration
The concentration of carbon dioxide that would cause the same radiative forcing as a given mixture of carbon dioxide and other forcing components. Those values may consider only greenhouse gases, or a combination of greenhouse gases and aerosols. Equivalent carbon dioxide concentration is a metric for comparing radiative forcing of a mix of different greenhouse gases at a particular time but does not imply equivalence of the corresponding climate change responses nor future forcing. There is generally no connection between equivalent carbon dioxide emissions and resulting equivalent carbon dioxide concentrations. (IPCC AR5 WGI Annex III: Glossary)

Eutrophication
Over-enrichment of water by nutrients such as nitrogen and phosphorus. It is one of the leading causes of water quality impairment. The two most acute symptoms of eutrophication are **hypoxia** (a state of oxygen depletion) and harmful algal blooms. (IPCC AR5 WGII Annex II: Glossary).

Extratropical cyclone
A large-scale (of order 1,000 km) storm in the middle or high latitudes having low central pressure and fronts with strong horizontal gradients in temperature and humidity. A major cause of extreme wind speeds and heavy precipitation especially in wintertime. (IPCC AR5 WGI Annex III: Glossary)

Feedbacks
An interaction between processes in the climate system, in which the result of an initial process triggers changes in a second process that in turn influences the initial one. A **positive feedback** magnifies the original process, while a **negative feedback** attenuates or diminishes it. Positive feedbacks are sometimes referred to as "vicious" or "virtuous" cycles, depending on whether their effects are viewed as harmful or beneficial. (*CSSR, Ch. 15*)

Geoengineering
A broad set of methods and technologies that aim to deliberately alter the climate system in order to alleviate the impacts of climate change (also known as **climate intervention** (National Academy of Sciences) or climate engineering). Most, but not all, methods seek to either 1) reduce the amount of absorbed solar energy in the climate system (**Solar Radiation Management**) or 2) increase net carbon sinks from the atmosphere at a scale sufficiently large to alter climate (**Carbon Dioxide Removal**). Scale and intent are of central importance. Two key characteristics of geoengineering methods of particular concern are that they use or affect the climate system (e.g., atmosphere, land, or ocean) globally or regionally and/or could have substantive unintended effects that cross national boundaries. (adapted from IPCC AR5 WGI Annex III: Glossary)

Glacial isostatic adjustment (GIA)
The deformation of the Earth and its gravity field due to the response of the earth–ocean system to changes in ice and associated water loads. It includes vertical and horizontal deformations of the Earth's surface and changes in geoid due to the redistribution of mass during the ice–ocean mass exchange. GIA is currently contributing to relative sea level rise in much of the continental United States. (IPCC AR5 WGI Annex III: Glossary)

Glacier
A perennial mass of land ice that originates from compressed snow, shows evidence of past or present flow (through internal deformation and/or sliding at the base), and is constrained by internal stress and friction at the base and sides. A glacier is maintained by accumulation of snow at high altitudes, balanced by melting at low altitudes and/or discharge into the sea. An ice mass of the same origin as glaciers, but of continental size, is an **ice sheet**, defined further below. (IPCC AR5 WGI Annex III: Glossary)

Global mean sea level
The average of relative sea level or of sea surface height across the ocean.

Global warming potential (GWP)
An index, based on radiative properties of greenhouse gases, measuring the radiative forcing following a pulse emission of a unit mass of a given greenhouse gas in the present-day atmosphere integrated over a chosen time horizon, relative to that of carbon dioxide. The GWP represents the combined effect of the differing times these gases remain in the atmosphere and their relative effectiveness in causing radiative forcing. (truncated from IPCC AR5 WGI Annex III: Glossary)

Gravimetry
Measurement of the Earth's gravitational field. Using satellite data from the Gravity Recovery and Climate Experiment (GRACE), measurements of the mean gravity field help scientists better understand the structure of the solid Earth and learn about ocean circulation. Monthly measurements of time-variable gravity can be used to study ground water fluctuations, sea ice, sea level rise, deep ocean currents, ocean bottom pressure, and ocean heat flux. (modified from *NASA Earth Observatory on the* GRACE *project*)

Greenhouse gas (GHG)
Greenhouse gases are those gaseous constituents of the atmosphere, both natural and anthropogenic, that absorb and emit radiation at specific wavelengths within the spectrum of terrestrial radiation emitted by the Earth's surface, the atmosphere itself, and by clouds. This property causes the greenhouse effect. Water vapor (H_2O), carbon dioxide (CO_2), nitrous oxide (N_2O), methane (CH_4), and ozone (O_3) are the primary greenhouse gases in the Earth's atmosphere. Moreover, there are a number of entirely human-made greenhouse gases in the atmosphere, such as the halocarbons and other chlorine- and

bromine-containing substances, dealt with under the Montreal Protocol. Beside CO_2, N_2O, and CH_4, the Kyoto Protocol dealt with the greenhouse gases sulfur hexafluoride (SF_6), hydrofluorocarbons (HFCs), and perfluorocarbons (PFCs). (adapted from IPCC AR5 WGI Annex III: Glossary)

Hydrological drought
See **drought**.

Hypoxia
Deficiency of oxygen in water bodies, which can be a symptom of **eutrophication** (nutrient overloading). **Deoxygenation** (the process of removing oxygen) leads to hypoxia, and the expansion of **oxygen minimum zones** (IPCC AR5 WGII Annex II: Glossary supplemented with other sources).

Ice sheet
A mass of land ice of continental size that is sufficiently thick to cover most of the underlying bed, so that its shape is mainly determined by its dynamics (the flow of the ice as it deforms internally and/or slides at its base). An ice sheet flows outward from a high central ice plateau with a small average surface slope. The margins usually slope more steeply, and most ice is discharged through fast flowing ice streams or outlet glaciers, in some cases into the sea or into ice shelves floating on the sea. There are only two ice sheets in the modern world, one on Greenland and one on Antarctica. During glacial periods there were others, including the Laurentide Ice Sheet in North America, whose loss is the primary driver of **glacial isostatic adjustment** in the United States today. (adapted from IPCC AR5 WGI Annex III: Glossary)

Ice wedge
Common features of the subsurface in permafrost regions, ice wedges develop by repeated frost cracking and ice vein growth over hundreds to thousands of years. Ice wedge formation causes the archetypal polygonal patterns seen in tundra across the Arctic landscape. (adapted from Liljedal et al., 2016)

Instantaneous radiative forcing
See **radiative forcing**.

Irreversible
Changes in components of the climate system that either cannot be reversed, or can only be reversed on timescales much longer than the timescale over which the original forcing occurred. (*CSSR, Ch. 15*)

Longwave cloud radiative effect (LWCRE)
See **cloud radiative effect**.

Meridional overturning circulation (MOC)
Meridional (north–south) overturning circulation in the ocean quantified by zonal (east–west) sums of mass transports in depth or density layers. In the North Atlantic, away from the subpolar regions, the Atlantic MOC (AMOC, which is in principle an observable quantity) is often identified with the thermohaline circulation (THC), which is a conceptual and incomplete interpretation. It must be borne in mind that the AMOC is also driven by wind, and can also include shallower overturning cells such as occur in the upper ocean in the tropics and subtropics, in which warm (light) waters moving poleward are transformed to slightly denser waters and subducted equatorward at deeper levels. (adapted from IPCC AR5 WGI Annex III: Glossary)

Meridional temperature gradient
North–South temperature variation

Meteorological drought
See **drought**.

Mode water
Water of exceptionally uniform properties over an extensive depth range, caused in most instances by convection. Mode waters represent regions of water mass formation; they are not necessarily water masses in their own right but contribute significant volumes of water to other water masses. Because they represent regions of deep sinking of surface water, mode water formation regions are atmospheric heat sources. Subantarctic Mode Water is formed during winter in the subantarctic zone just north of the subantarctic front and contributes to the lower temperature range of central water; only in the extreme eastern Pacific Ocean does it obtain a temperature low enough to contribute to Antarctic Intermediate Water. Subtropical

Mode Water is mostly formed through enhanced subduction at selected locations of the subtropics and contributes to the upper temperature range of central water. Examples of Subtropical Mode Water are the 18°C water formed in the Sargasso Sea, Madeira Mode Water formed at the same temperature but in the vicinity of Madeira, and 13°C water formed not by surface processes but through mixing in Agulhas Current eddies as they enter the Benguela Current. (AMS glossary).

Model ability/model skill
Representativeness of the ability of a climate model to reproduce historical climate observational data.

Model bias
Systematic error in model output that over- or under-emphasizes particular model mechanism or results.

Model ensemble
Also known as a multimodel ensemble (MME), a group of several different global climate models (GCMs) used to create a large number of climate simulations. An MME is designed to address **structural model uncertainty** between different climate models, rather than **parametric uncertainty** within any one particular model. (*UK Met Office, Climate Projections*, Glossary)

Model independence
An analysis of the degree to which models are different from one another. Also is used as an interpretation of an ensemble as constituting independent samples of a distribution which represents our collective understanding of the climate system. (summarized based on Annan and Hargreaves, 2017)

Nationally determined contributions (NDCs)
See **Paris Agreement**.

Negative feedbacks
See **feedbacks**.

Nitrogen mineralization
Mineralization/remineralization is the conversion of an element from its organic form to an inorganic form as a result of microbial decomposition. In nitrogen mineralization, organic nitrogen from decaying plant and animal residues (proteins, nucleic acids, amino sugars and urea) is converted to ammonia (NH_3) and ammonium (NH4+) by biological activity. (IPCC AR5 WGI Annex III: Glossary)

Ocean acidification
The process by which ocean waters have become more acidic due to the absorption of human-produced carbon dioxide, which interacts with ocean water to form carbonic acid and lower the ocean's pH. Acidity reduces the capacity of key plankton species and shelled animals to form and maintain shells. (*USGCRP*)

Ocean stratification
The existence or formation of distinct layers or laminae in the ocean identified by differences in thermal or salinity characteristics (e.g., densities) or by oxygen or nutrient content. (adapted from AMS glossary).

Oxygen minimum zones (OMZs)
The midwater layer (200–1,000 m) in the open ocean in which oxygen saturation is the lowest in the ocean. The degree of oxygen depletion depends on the largely bacterial consumption of organic matter, and the distribution of the OMZs is influenced by large-scale ocean circulation. In coastal oceans, OMZs extend to the shelves and may also affect benthic ecosystems. OMZs can expand through a process of **deoxygenation**. (supplemented version of IPCC AR5 WGII Annex II: Glossary).

Pacific Decadal Oscillation
The pattern and time series of the first empirical orthogonal function of sea surface temperature over the North Pacific north of 20°N. The PDO broadened to cover the whole Pacific Basin is known as the Interdecadal Pacific Oscillation. The PDO and IPO exhibit similar temporal evolution. (IPCC AR5 WGI Annex III: Glossary)

Parameterization
In climate models, this term refers to the technique of representing processes that cannot be explicitly resolved at the spatial or temporal resolution of the model (sub-grid scale processes) by relationships between model-resolved

larger-scale variables and the area- or time-averaged effect of such subgrid scale processes. (IPCC AR5 WGI Annex III: Glossary)

Parametric uncertainty
See **uncertainty**.

Paris Agreement
An international climate agreement with the central aim to hold global temperature rise this century well below 2°C above preindustrial levels and to pursue efforts to limit the temperature increase even further to 1.5°C. For the first time, all parties are required to put forward emissions reductions targets, and to strengthen those efforts in the years ahead as the Agreement is assessed every five years. Each country's proposed mitigation target (the intended nationally determined contribution [INDC]) becomes an official **nationally determined contribution (NDC)** when the country ratifies the agreement. The Paris Agreement was finalized on December 12, 2015, at the 21st Conference of Parties (COP 21) of the United National Framework Convention on Climate Change (UNFCCC). "Paris" entered into force on November 4, 2016, after ratification by 55 countries that account for at least 55% of global emissions). The agreement had a total of 125 national parties by early 2017. (summarized/edited from *UNFCCC*)

Pattern scaling
A simple and computationally cheap method to produce climate projections beyond the scenarios run with expensive global climate models (GCMs). The simplest technique has known limitations and assumes that a spatial climate anomaly pattern obtained from a GCM can be scaled by the global mean temperature anomaly. (Herger et al., 2015)

Permafrost
Ground that remains at or below freezing for at least two consecutive years. (*USGCRP*)

Permafrost active layer
The layer of ground that is subject to annual thawing and freezing in areas underlain by permafrost. (IPCC AR5 WGI Annex III: Glossary)

Petagram
One petagram (Pg) = 10^{15} grams or 10^{12} kilograms. A petagram is the same as a gigaton, which is a billion metric tons, where 1 metric ton is 1,000 kg. Estimated 2014 global fossil fuel emissions were 9.855 Pg = 9.855 Gt = 9,855 million metric tons of carbon. (CDIAC – Carbon Dioxide Information Center: Boden et al., 2017)

Positive feedbacks
See **feedbacks**.

Proxy
A way to indirectly measure aspects of climate. Biological or physical records from ice cores, tree rings, and soil boreholes are good examples of proxy data. (*USGCRP*)

Radiative forcing
The change in the net (downward minus upward) radiative flux (expressed in $W/m^{2)}$ at the tropopause or top of atmosphere due to a change in an external driver of climate change, such as a change in the concentration of carbon dioxide or in the output of the Sun. Sometimes internal drivers are still treated as forcings even though they result from the alteration in climate, for example aerosol or greenhouse gas changes in paleoclimates. The traditional radiative forcing is computed with all tropospheric properties held fixed at their unperturbed values, and after allowing for stratospheric temperatures, if perturbed, to readjust to radiative–dynamical equilibrium. Radiative forcing is **instantaneous** if no change in stratospheric temperature is accounted for. The radiative forcing once rapid adjustments are accounted for is the **effective radiative forcing**. Radiative forcing is not to be confused with cloud radiative forcing, which describes an unrelated measure of the impact of clouds on the radiative flux at the top of the atmosphere. (truncated from IPCC AR5 WGI Annex III: Glossary)

Relative sea level
The height of the sea surface, measured with respect to the height of the underlying land. Relative sea level changes in response to both changes in the height of the sea surface and changes in the height of the underlying land.

Representative Concentration Pathways
Scenarios that include time series of emissions and concentrations of the full suite of greenhouse gases and aerosols and chemically active gases, as well as land use/land cover. The word "representative" signifies that each RCP provides only one of many possible scenarios that would lead to the specific radiative forcing characteristics. The term "pathway" emphasizes that not only the long-term concentration levels are of interest, but also the trajectory taken over time to reach that outcome. RCPs usually refer to the portion of the concentration pathway extending up to 2100. Four RCPs produced from Integrated Assessment Models were selected from the published literature for use in the Intergovernmental Panel on Climate Change's Fifth Assessment Report: **RCP2.6**, a pathway where radiative forcing peaks at approximately 3 W/m^2 before 2100 and then declines; **RCP4.5** and **RCP6.0**, two intermediate stabilization pathways in which radiative forcing is stabilized at approximately 4.5 W/m^2 and 6.0 W/m^2, respectively, after 2100; and **RCP8.5**, a high pathway for which radiative forcing reaches greater than 8.5 W/m^2 by 2100 and continues to rise for some amount of time (truncated and adapted from IPCC AR5 WGI Annex III: Glossary, excluding discussion of extended concentration pathways)

Rossby waves
Rossby waves, also known as planetary waves, naturally occur in rotating fluids. Within the Earth's ocean and atmosphere, these waves form as a result of the rotation of the planet. These waves affect the planet's weather and climate. Oceanic Rossby waves are huge, undulating movements of the ocean that stretch horizontally across the planet for hundreds of kilometers in a westward direction. Atmospheric Rossby waves form primarily as a result of the Earth's geography. Rossby waves help transfer heat from the tropics toward the poles and cold air toward the tropics in an attempt to return the atmosphere to balance. They also help locate the jet stream and mark out the track of surface low pressure systems. The slow motion of these waves often results in fairly long, persistent weather patterns. (adapted from NOAA National Ocean Service)

Saffir-Simpson hurricane scale
A classification scheme for hurricane intensity based on the maximum surface wind speed and the type and extent of damage done by the storm. The wind speed categories are as follows: 1) 33–42 m/s (65–82 knots or 74–95 mph); 2) 43–49 m/s (83– 95 knots or 96–110 mph); 3) 50–58 m/s (96–113 knots or 111–129 mph); 4) 59–69 m/s (114–134 knots or 130–156 mph); and 5) 70 m/s (135 knots or 156 mph) and higher. These categories are used routinely by weather forecasters in North America to characterize the intensity of hurricanes for the public. (adapted from AMS glossary).

Saturation
The condition in which vapor pressure is equal to the equilibrium vapor pressure over a plane surface of pure liquid water, or sometimes ice. (AMS glossary).

Scenarios
Plausible descriptions of how the future may develop based on a coherent and internally consistent set of assumptions about key driving forces (e.g., rate of technological change, prices) and relationships. Note that scenarios are neither predictions nor forecasts, but are useful to provide a view of the implications of developments and actions. (IPCC AR5 WGI Annex III: Glossary)

Sea level pressure
The atmospheric pressure at mean sea level, either directly measured or, most commonly, empirically determined from the observed station pressure. In regions where the Earth's surface is above sea level, it is standard observational practice to reduce the observed surface pressure to the value that would exist at a point at sea level directly below if air of a temperature corresponding to that actually present at the surface were present all the way down to sea level. In actual practice, the mean temperature for the preceding 12 hours is employed, rather than the current temperature. This "reduction of pressure to sea level" is responsible for many anomalies in the pressure field in mountainous areas on the surface synoptic chart. (AMS glossary).

Shared Socioeconomic Pathways
A basis for emissions and socioeconomic scenarios, an SSP is one of a collection of pathways that describe alternative futures of socioeconomic development in the absence of climate policy intervention. The combination of SSP-based socioeconomic scenarios and **Representative Concentration Pathway (RCP)**-based climate projections can provide a useful integrative frame for climate impact and policy analysis. (updated from IPCC AR5 WGIII Annex I: Glossary).

Shortwave cloud radiative effect (SWCRE)
See **cloud radiative effect**.

Snow water equivalent
The depth of liquid water that would result if a mass of snow melted completely. (IPCC AR5 WGI Annex III: Glossary)

Solar radiation management (SRM)
The intentional modification of the Earth's shortwave radiative budget with the aim to reduce climate change according to a given metric (for example, surface temperature, precipitation, regional impacts, etc). Artificial injection of stratospheric aerosols and cloud brightening are two examples of SRM techniques. Methods to modify some fast-responding elements of the longwave radiative budget (such as cirrus clouds), although not strictly speaking SRM, can be related to SRM. See also **geoengineering**. (edited from IPCC AR5 WGI Annex III: Glossary)

Static-equilibrium (sea level change) fingerprint
The near-instantaneous pattern of **relative sea level** change associated with changes in the distribution of mass at the surface of the Earth, for example due to the melting of ice on land. Near a shrinking ice sheet (within ~2,000 km of the margin), sea level will fall due to both crustal uplift and the reduction of the gravitational pull on the ocean from the ice sheet. Close to the ice sheet, this fall can be an order of magnitude greater than the equivalent rise in global mean sea level associated with the meltwater addition to the ocean. Far from the ice sheet, sea level will generally rise with greater amplitude as the distance from the ice sheet increases, and this rise can exceed the global mean value by up to about 30%. (draws on Hay et al., 2012)

Structural model uncertainty
See **uncertainty**.

Teleconnection
A statistical association between climate variables at widely separated, geographically fixed spatial locations. Teleconnections are caused by large spatial structures such as basin-wide coupled modes of ocean–atmosphere variability, Rossby wave-trains, midlatitude jets and storm tracks, etc. (IPCC AR5 WGI Annex III: Glossary)

Thermohaline circulation (THC)
Large-scale circulation in the ocean that transforms low-density upper ocean waters to higher-density intermediate and deep waters and returns those waters back to the upper ocean. The circulation is asymmetric, with conversion to dense waters in restricted regions at high latitudes and the return to the surface involving slow upwelling and diffusive processes over much larger geographic regions. The THC is driven by high densities at or near the surface, caused by cold temperatures and/or high salinities, but despite its suggestive though common name, is also driven by mechanical forces such as wind and tides. Frequently, the name THC has been used synonymously with the **Meridional Overturning Circulation**. (IPCC AR5 WGI Annex III: Glossary)

Thermokarst
The process by which characteristic landforms result from the thawing of ice-rich permafrost or the melting of massive ground ice. (IPCC AR5 WGI Annex III: Glossary)

Threshold
The value of a parameter summarizing a system, or a process affecting a system, at which qualitatively different system behavior emerges. Beyond this value, the system may not conform to statistical relationships that described it previously. For example, beyond a threshold level of ocean acidification, wide-scale collapse of coral ecosystems may occur. (*CSSR, Ch. 15*)